Journal of
ENGINEERING in Medical Devices

TEC | Tecnológico de Costa Rica

VOL. II, OCTOBER 2017 - MARCH 2018 • ISSN: 2215-4914

OFFICIAL JOURNAL OF MEDICAL DEVICES ENGINEERING IN COSTA RICA
SCHOOL OF MATERIALS SCIENCE AND ENGINEERING • COSTA RICA INSTITUTE OF TECHNOLOGY (TEC)

CREDITS

This journal – the first of its kind in Costa Rica - showcases the work of students and faculty carried out as part of the focal point for scholarly basic and applied research on materials in the medical device field. Works carried out outside of the program on related topics are also welcome to submit a contribution.

Journal of ENGINEERING in Medical Devices

EDITOR´S OFFICE

Phone (506) 2550-2704/ 2550-2213
P.O.Box: 159 7050
Cartago, Costa Rica

DESIGN AND PRINT

Unidad de Publicaciones TEC

Main cover caption: Process followed for the design of a cleft lip and cleft palate device: using different 3D technologies to capture the face of an infant, a model with the features of the face can be constructed, from which a customized device can be designed and then prototyped. Images courtesy of Gustavo Rojas-Soto, David De Faria-Castro, Miceldy Rios-Sanabria, Victor Carmona-Infante, from the contribution: **MEDICAL DEVICE FOR TREATMENT OF CLEFT LIP AND CLEFT PALATE AFTER SURGICAL PROCEDURE** included in this issue.

TEC | Tecnológico de Costa Rica

Journal of ENGINEERING in Medical Devices

Contents

Academic tools for the challenges of the future

Costa Rica has gained, with the passing of the years, a recognized name around the world as a strategic destination for investments with high added value in one of the most dynamic sectors, as is the Life Sciences. This is without a doubt one of the fastest growing sectors promoted by CINDE for the attraction of foreign direct investment of multinational companies.

Today, six out of the ten most important companies in the world in the cardiovascular sector are operating from Costa Rica, which are also part of 70 multinational companies in the medical devices sector that reported exports in 2016 of the sum of US $2,500 million and generated employment to more than 21,000 Costa Ricans.

In this context, the Master's Degree in Medical Device Engineering, a driven initiative from the Instituto Tecnológico de Costa Rica (TEC), the University of Minnesota and CINDE, is vital to meet the demand of professionals that these companies are requiring, and to expose our human resources to the new educational trends that set the standard around the world.

The challenge for the future of Costa Rica is to achieve that the academic sector responds to global transformation, as TEC has been doing. The Master Program in Medical Device Engineering is a first initiative, and gradually more academic initiatives will have the challenge of complying with standards and specialization required with an industry in constant transformation.

Vanessa Gibson, Manager of Investment Climate

Costa Rican Investment Promotion Agency (CINDE).

Journal of ENGINEERING in Medical Devices

In this second issue of the Journal of Engineering in Medical Devices, new contributions from work carried out during the Graduate Program in Medical Devices Engineering of the Costa Rica Institute of Technology are presented with great satisfaction from the Editorial Committee. For example, the Materials Characterization class, which provided original papers for the **Academic Focus** section, shows incredible progress has been achieved in acquiring new equipment and in know-how for failure analysis of materials, determination of structure and chemical composition, and structure – property relationships. Different kinds of materials such as polymers (Nylon and EVA) and metals (Titanium and Stainless Steel) were characterized to address quality issues or gain knowledge about the material.

In the **Applied Engineering** section, two completely innovative designs for medical devices, conceptualized from the graduation work of students, are presented. It is important to highlight the focus on prototyping and testing of these devices on real situations with the recommendation from physicians. The use of additive manufacturing techniques has a lot of value added to the design work.

In the **Technical Notes** section, an interesting work on simulation of severe plastic deformation techniques for processing of biomedical titanium alloys is shown, with great potential for development of interesting processes for manufacturing of medical device components. Simulation is a hot field in research and development groups of the medical device companies.

Finally, I would like to remind the readership of this journal that contributions from industry and academia that fit the scope of the journal are welcome to submit a paper.

Also, we once more acknowledge all the contributors, supervisors and reviewers for their hard work in providing the content of this issue. We expect to match the expectation of our readership and improve the quality of the contributions with time.

Jorge M. Cubero Sesin, Ph.D.
Editorial Director
jcubero@itcr.ac.cr

MEDICAL DEVICE FOR TREATMENT OF CLEFT LIP AND CLEFT PALATE AFTER SURGICAL PROCEDURE

Gustavo Rojas-Soto[1], David De Faria-Castro[2], Miceldy Rios-Sanabria[3], Victor Carmona-Infante[4]

Received: June 15th, 2017

Accepted: September 18th, 2017

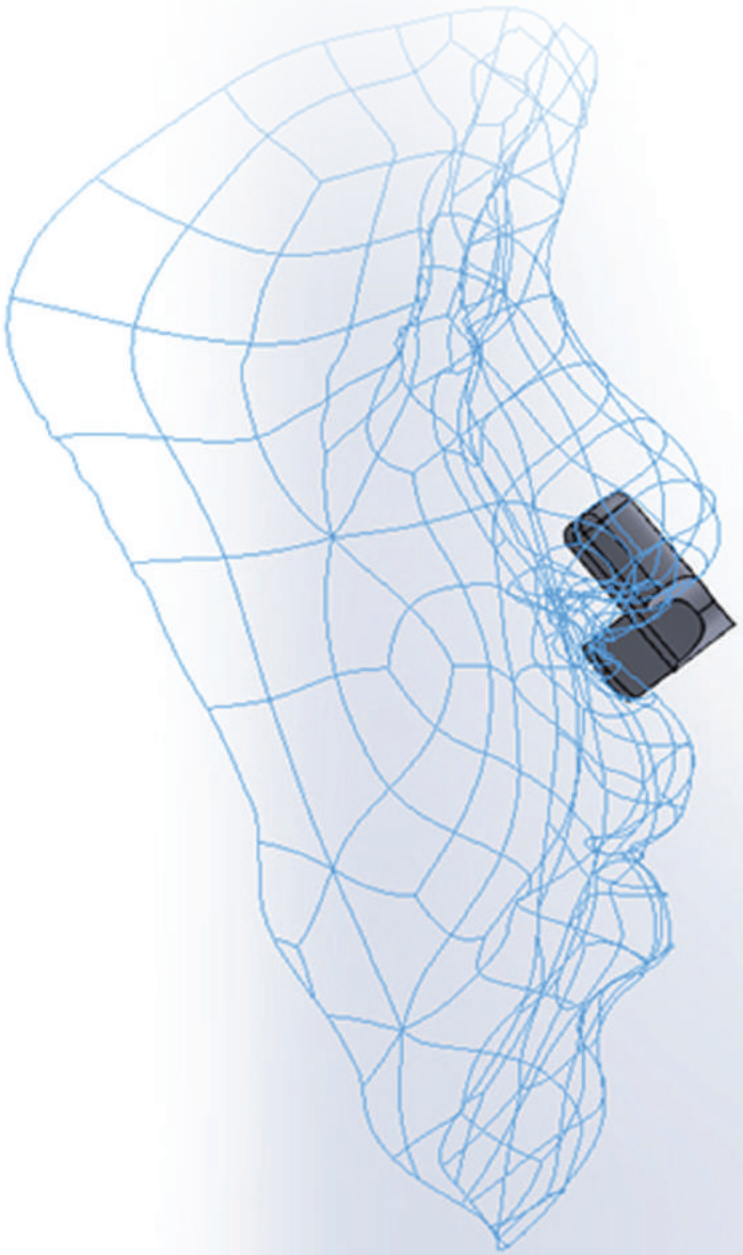

1 Electronic Engineer, ICU Medical, Costa Rica, gustavo.rojas.soto@gmail.com

2 Industrial Design Engineer, Procomer, Costa Rica, ddefaria@procomer.com

3 Electromechanical Engineer, Cooper Surgical, Costa Rica, riosmiceldy@gmail.com

4 Biotechnology Engineer, Philips, Costa Rica, vikwolfp@gmail.com

Journal of ENGINEERING in Medical Devices

ABSTRACT

The Cleft Lip and Cleft Palate condition has a low incidence in the population, between 0.014 and 0.2% of births worldwide. However, this illness requires that the patients undergo several surgeries throughout their life; therefore, it has a high impact at physiological and psychological level. The devices normally used are not effective because they offer little ergonomic support, which causes damage to tissues and allergies on infants who are attending on pre-surgical and post-surgical treatments, causing a less positive effect of the treatment. The project is intended to design a proposal post-surgical support device for treatment of cleft lip and cleft palate. The determination of design requirements was detected by interviewing doctors and parents. Subsequently, different 3D technologies were used to capture the face of an infant with the condition and final three proposal devices were modeled. The prototypes were constructed with three different printers and materials, the best result was found by using the PA 2200 material on the EOSINT P 730 printer. The results showed that two out of three devices were well-welcomed by the interviewers, noting that one could be used during the day and the other one at night.

RESUMEN

El padecimiento de labio leporino y paladar hendido posee una baja incidencia en la población, entre 0.014% y 0.2% de los nacimientos a nivel mundial. Sin embargo, el paciente que posee la condición debe someterse a varias intervenciones quirúrgicas a lo largo de su vida. Actualmente, se emplean soportes poco ergonómicos que provocan daño en los tejidos y alergias en los infantes atendidos en los tratamientos pre y post quirúrgicos, causando un efecto no tan positivo en el tratamiento. El proyecto busca diseñar una propuesta para un dispositivo de soporte post quirúrgico para el tratamiento de labio leporino y paladar hendido. Las determinaciones de los requerimientos de diseño se detectaron por medio de encuestas a médicos y padres de familia; seguidamente, se emplearon diferentes tecnologías 3D para capturar el rostro de un infante con el padecimiento; después, se prosiguió a modelar las tres propuestas finales de dispositivo. Los prototipos se imprimieron con tres diferentes impresoras y materiales, el mejor acabado se obtuvo empleando como material el PA 2200 en la impresora EOSINT P 730. Los resultados mostraron que dos de los tres dispositivos fueron aceptados por los entrevistados, señalando que uno podría ser usado durante el día y el otro durante la noche.

Keywords:

Cleft Lip, Cleft Palate, 3D technologies, 3D images, medical device, prototyping.

Palabras clave:

labio leporino, labio paladar hendido, tecnologías en 3D, imágenes 3D, dispositivo médico, prototipado.

Introduction:

Cleft lip and cleft palate (CL&CP) are disruptions immediately present on the face structure. This disease has an incidence of infant mortality in children from third world countries [1]. The patient with cleft lip and cleft palate suffers problems in speaking, feeding, listening and social integration, among others. These facial and oral malformations can be corrected through several surgeries, dental treatment, speech therapy and psychological support [1].

The most common patterns of CL&CP involve a physical separation of the two sides of the upper lip, spreading inside the nostrils and/or palate (hard and soft tissues). Studies about the malformation have mentioned that the indents which imply backwards structures (clef lip and cleft palate), could be originated due to genetic and embryological matters involving only the secondary palate. Although there are a lot of disorders that affect all the craniofacial tissues, the overwhelming majority involves the upper lip and/or the palate [1].

Cleft lip and cleft palate requires surgical treatments with the objective to improve the aesthetics of patients, eliminate the difficulty to eat, speaking issues, occlusion, crossed bite and lost teeth [2]. These surgical procedures are performed between three and four months of patients' age to produce the join of their lips; afterwards, a surgery is done to close the mouth roof separation between 18 to 24 months of age. Depending on the severity of the malformation the patient could need more surgeries [3].

Some countries have in place a pre-surgery treatment that is a passive method called nosealveolar molding [4]. This method joins the lip and the alveolus applying force through the direction of growth. The main goal of this treatment is to reduce the severity of the initial deformity and improve long-term nasal symmetry before the corrective surgery.

Post-surgery deformities of one-sited and two-sided cleft lip and cleft palate are common on patients. In several cases, this situation occurs due to the tissues and skin softness, incorrect surgery planning or delayed surgeries [5]. Examples of deformities post-surgery are shown in Figure 1.

Figure 1. Deformities present on patients after surgeries of cleft lip and cleft palate [6].

Generally, two types of devices are used to correct the nose misalignment: passive and active devices. Active devices are fixed in the intraoral way pulling the tissues through mechanical forces using elastic chains, screws and plates (Figure 2a). Passive devices maintain the distance between the maxillary segments, whereas the external force is applied to change the rear position. The device of nose alveolar molding (Figure 2b) is a well elaborated passive device which consists in an acrylic plate intraoral fixed with elastic extraorals and glue tape. Wire stabilizers are added to apply force prolonging the vestibule of the nostrils and elongation of the nose columella.

A)

B)

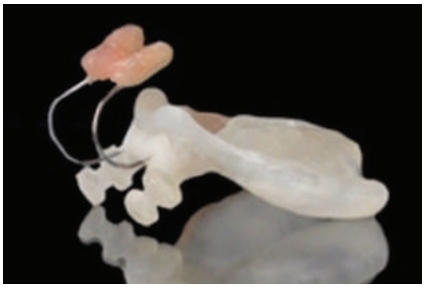

Figure 2. Examples of devices normally used on patients. A) External Maxillary Support. B) Molding Nosealveolar Device [3].

Journal of ENGINEERING in Medical Devices

The current study is intended to develop a prototype of an ergonomic medical device for the treatment of cleft lip and cleft palate on post-surgery patients by 3D technologies using different printers and materials.

Materials and methods

In general terms, the model used to develop this medical device follows the design control FDA proposal to assure that the specific design requirements were met as requested by the FDA el 21CFR 820.3 [6]. It is observed in Figure 3 that the design phases are an activate cycle in which there is a constant revision of the results, and those results will serve as input requirements for the next one. That verification and validation processes should be used to ensure compliance with design and use requirements respectively [7,8].

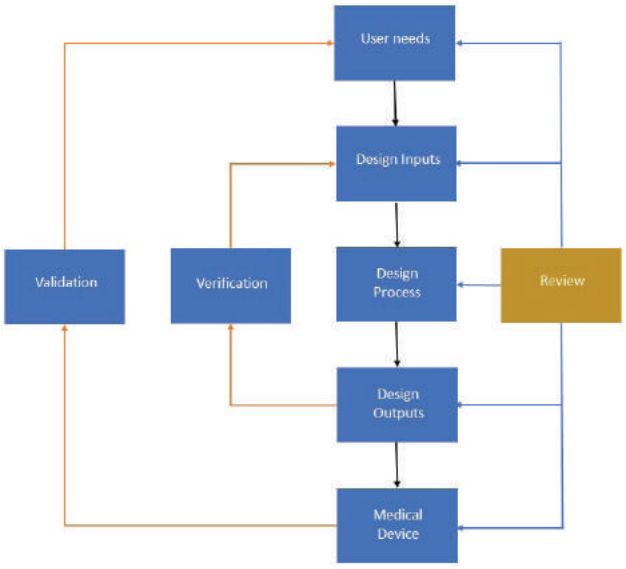

Figure 3. Phases of control design, diagram based on the FDA control design guide [7].

For the development of this process it was necessary to obtain the specifications of the product throughout surveys to internal medicine specialists and maxillofacial surgery, also to the parents and experts in the post-surgical treatment (The Association Pro Child with Cleft lip and Cleft Palate are experts in the post-operative treatment). It was identified that the designs must be ergonomic and functional by providing support to the nasal septum. Moreover, it should be aesthetically attractive to have the infant wearing it for as long as possible. Additionally, the device must be capable to adapt to the patient so that there are the least amount of usage restrictions and to have a user-friendly interface.

For obtaining a three-dimensional image of an infant with the condition, three tests were made with three different technologies to capture the image that can be used for the device design. The technologies used were the ItSeez3D app, 123D Catch app and the software Design X that uses the scanner REVScan of Creaform. Later, the prototype design was made using SolidWorks® software from Dassault Systems.

In order to have physical prototypes to show to the parents, doctors and experts, and to obtain their feedback, it was necessary to obtain 3D impressions of them. A print service search was performed, each service used a compatible material with the 3D printer model. PC-ABS plastic on a Stratasys Fortus 360mc printer, Ninja-Flex material with a Printrbot printer and PA 2200 polymer on EOSINT P730 printer were used.

Results

First, the ItSeez3D app was used which required a mobile device (tablet or cell phone) to capture the 3D image of the object (Figure 4a); however due to its low resolution and that the infant could not keep still for the required time, a digital file could not be used for modelling. With the 123D Catch app, a better resolution was obtained (Figure 4b), in which a series of digital photographs captured from different angles to generate the 3D image are superimposed. Despite of having a better resolution while the infant remained asleep, the result was still far from the requirements to be employed in the design software. Finally, the software Design X that uses the scanner REVScan of Creaform generated an image with the resolution of surface that was

adequate to be used in the design of the devices (Figure 4c).

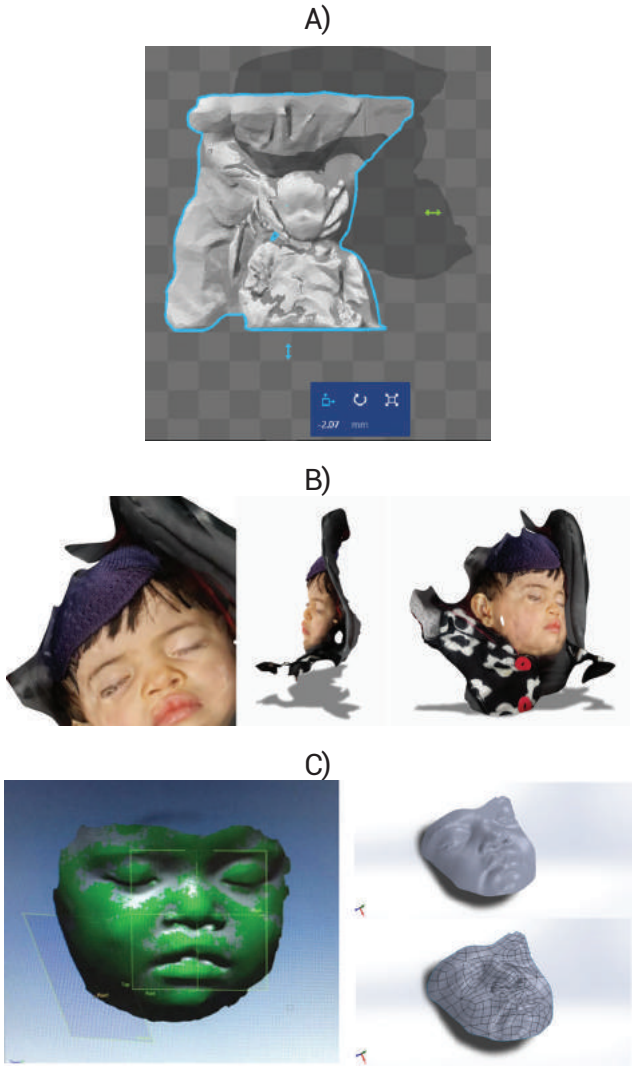

Figure 4. Scanning image of a child with CL&CP from a) ItSeez3D app, b) 123D Catch app and c) Design X software.

Prototype design was used to identify the patient's nostrils and the dimensions of the device based on the size, then added the point of force for the base of the nose. This process was used for the development of the three device proposals: basal support, front support and column support, names chosen by the point where the force of subjection to the nasal septum is generated, as illustrated and identified in Figure 5A, B and C, respectively.

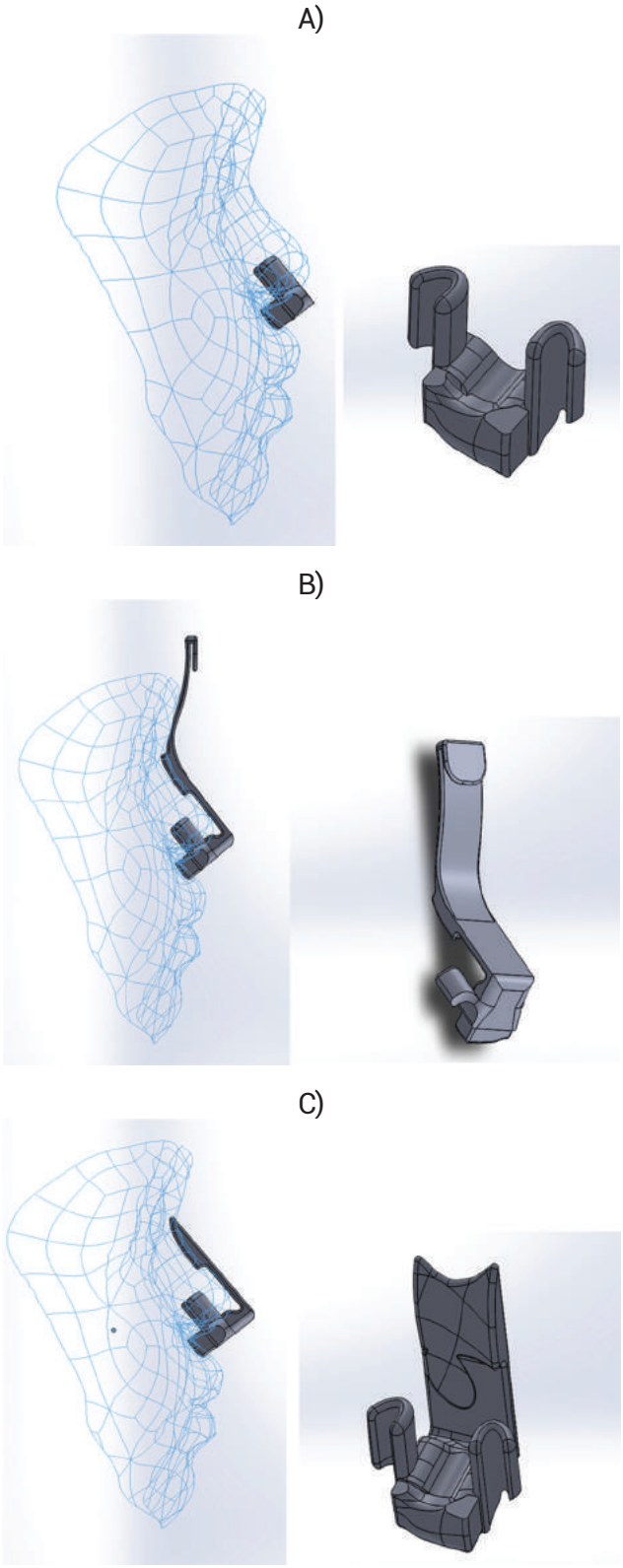

Figure 5. Three proposal prototype created in SolidWorks® software. A) Basal support. B) Front support. C) Support Column.

Journal of ENGINEERING in Medical Devices

Figure 5 shows the different results for the prototype of Basal Support, to the nose, rigid but at the same time flexible enough to provide an ergonomic interface with the user. Figure 6a shows the impression obtained with a PC-ABS plastic on a Stratasys Fortus 360mc printer, the material is rigid and produced that the device break easily during handling. In contrast, using the Ninja-Flex material with a Printrbot printer (Figure 5b), the device was too flexible and with a very porous surface finish, that it could not confer support to the nasal septum. Finally, using a PA 2200 polymer on EOSINT P730 printer, the desired finishing in prototype was obtained with rigidity and balanced flexibility to be used in testing and data collection of the focus group (Figure 5c).

A)

B)

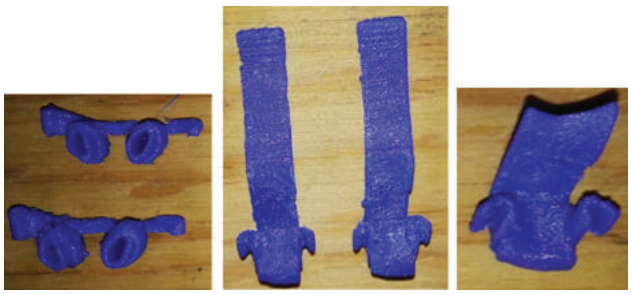

C)

Figure 6. Results of different 3D printing technologies in the Front Support. A) PC-ABS plastic on a Stratasys Fortus 360mc printer. B) Ninja-Flex with a Printrbot printer. C) PA 2200 polymer on an EOSINT P730 printer.

The prototype impressions were shown to the focus group and experts to evaluate the product specifications, previously identified for the three proposals against the current device position (Figure 2a). The experts who participated in the evaluation process of the medical devices proposal were parents of infants with the condition, an Internist and a Maxillofacial Surgeon, and the members of the Pro Niño Clef lip and Cleft Palate Association. Each person gave a score of 1 to 5, providing the maximum rating of 5 if the prototype reached 100% the desired requirement, this was done for each of the specifications and for each prototype and for the current device. Figure 7 shows how the Basal Support prototype got the highest score in all product specifications, followed by Frontal Support, thirdly the prototype of Column Support and finally, the current device.

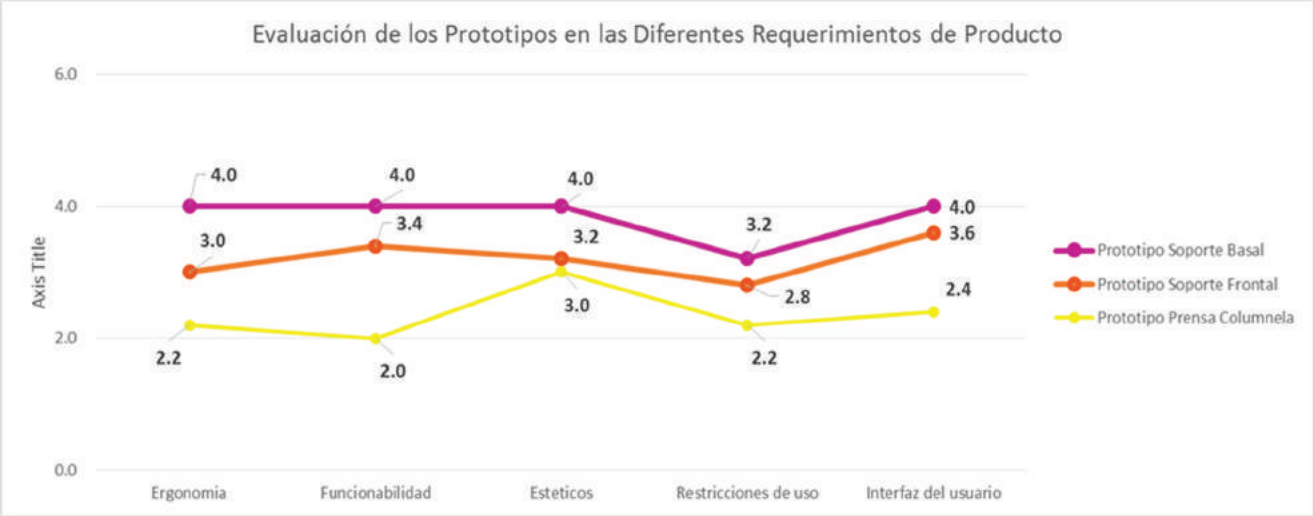

Figure 7. Evaluation of product requirements by prototype.

Discussion of results

The current nasal support used in these patients is uncomfortable and unsafe for the infant. This creates the necessity to develop a new ergonomic and safe device to allow patients to use it for different periods of time. Thus, providing the corrective reinforcement required to align the patient's facial features.

The 123D Catch and ItSeez3D scanning programs did not provide the level of detail required for an ergonomic development of nasal support. However, Creaform's REVscan System, using the VXElements program, provided the level of resolution and precision required to be used as the basis for nasal support design. However, it is a challenge to keep the patient immobile for the five minutes required to perform the scan.

There were several factors that could influence the scan result; for example, the individual to be scanned was asleep and immobile during scanning with the REVscan and 123D catch, while in scanning with ItSeez3D, the individual was awake and in constant motion, so the program cannot generate the required definition. The technologies 123D catch and ItSeez3D are limited by being a technology of superposition of photographs in different perspectives of an object, whereas the REVscan generates a cloud of points that allows it to generate greater precision and resolution of the object scanned.

In addition, 3D printing using the EOSINT P 730 material, proved to be the ideal technology for the manufacturing of nasal supports because of its precision, multi-material printing capability, moldability and low cost. When analyzing the three impressions obtained, the use of rigid materials such as PC-ABS for the printing of the nasal support, including the printing of the prototypes, was ruled out because of the lack of physical properties, such as the flexibility and superficial softness that favor the ergonomics of the device and patient safety. The Ninja Flex polymer is very soft, does not provide the necessary reinforcement to correct the post-surgery condition. This balance between flexibility and rigidity, which allows to have the corrective reinforcement but also the ergonomics for the treatment, was obtained with the material PLA 2200, achieving greater ergonomics and comfort in the patient for prolonged use.

The most accepted prototype for the corrective treatment of CL&CP is the basal support device, because this device has the smaller volume and fewer areas of contact with the patient, which makes it the most comfortable support and at the same

Journal of ENGINEERING in Medical Devices

time, has fewer fixing points. It makes the support less stable and easier to remove. Among the results of the interviews, it was suggested the use of this device in adolescents, young adults and adults and population with awareness of the necessity of using this device.

The specialist in maxillofacial surgery suggested different technologies, such as dental tomography to get the inside of the nostrils and for a fast digitization and good resolution "3DM phase" technology. Besides that, the surgeon proposed the use of a 3D projection of the patient, to generate several devices that sequentially correct the condition after the first surgical procedure.

The prototype of the frontal support was the second most accepted device. The internist doctors found that it was the best design to treat the target population of the study and gave the recommendation that the band that will attach the prototype to the head should take advantage of the irregularities of the head and even the ears to provide greater support in correcting the nasal septum. Since this device has two protrusions (which have sharp shapes) that allow it to attach to the upper part of the nose. Because it is close to the eyes, this makes the device the least safe for patients.

The last prototype evaluated was the prototype column support, this device was the least accepted, because its design has several sharp ends, despite that it is not ruled out its use in ages older than 5 years, since having two points of support and two of fixation, allows for better fixation in the nasal support, which is ideal to avoid being removed consciously or unconsciously by the patient. At the same time, this is the support with the greatest volume and visual impact on the patient face.

The results show that the three proposed prototypes are likely to be used in the post-surgical treatment of patients with CL&CP, but their use will depend on slight modifications in designs, the choice of hypoallergenic materials and the patient's maturity, therefore, all three devices could be used in different statistical populations of patients with CL&CP.

As recommendations, to use high-resolution scanning and printing technologies, the scanning method must have the ability to obtain the internal dimensions of the nostrils to improve the adaptability and effectiveness of the treatment.

For future work, it is important to develop devices that allow a gradual adjustment of nasal alignment; making the use of simulation software for progressive correction, as well as the 3D printing of a set of exchange devices over time until reaching the expected final form.

Finally, it is important to work together with the National Council for Biomedical Research (CONIS) with the objective of planning, approving and executing clinical studies with patients with cleft lip and cleft palate.

Conclusions

- ✓ Devices that were investigated to assist in the corrective treatment of cleft lip and cleft palate in nasal correction do not have design criteria; also, do not have fully documented acceptance criteria to know the patient's needs, representing a health risk and low corrective effectiveness.
- ✓ The Geomagic Design X software through the REVSCAN capture device presented the best resolution and surface modeled required in 3D of the patient, but it has the disadvantage that it is necessary for the patient to remain still and with eyes closed during the scan time.
- ✓ The combination of PA 2200 with the 3D printer EOSINT P 730 presented the best result in the manufacturing of the three prototypes in terms of surface finish, appearance and precision, however it is not the optimum material for the final version of the device.
- ✓ Of the three prototypes designed (Basal Support, Nasal Support, Columnar Support), the Basal Support device joins the most needs of the patient.

References

[1] Dixon, M.J., Marazita, M.L., Beaty T.H., Murray, J.C. (2011) Cleft lip and palate: understanding genetic and environmental influences. *Nature Reviews,* 12(3), 167-178.

[2] Ringdahl L. (2011). *The Long-term effect of nosealveolar molding on midface Growth and nasolabial esthetics in complete unilateral cleft lip and palate patients.* Master's thesis. Nova Southeastern University. Retrieved from NSU-Works, College of Dental Medicine.

[3] Cohen, M. (2004). Residual deformities after repair of clefts of the lip and palate. *Clin Plastic Surg* 31, 331-345.

[4] Grayson, B. D., Maull, D. (2005). Nasoalveolar Molding for infants born with cleft of the lip, Alveolus, and Palate. *Semi Surg.*, 19(4), 294-301.

[5] Mars, M., Plint, D.A., Houston, W.J., Bergland, O., Semb, G. (1987) The Goslon Yardstick: A new system of assessing dental arch relationships in children with unilateral clefts of the lip and palate. *The Cleft Palate Journal*, 24, 314-322.

[6] Food and Drug Administration. (2015). *CFR-Code of Federal Regulations, medical devices, part 820 Quality System Regulation, Sec. 820.30 Design Controls*. Recovered from https://www.accessdata.fda.gov/scripts/cdrh/cfdocs/cfCFR/CFRSearch.cfm?fr=820.30

[7] Weck, O., Wallace, P., Young, P., Yong Kim. *"A Rewarding CAD / CAE / CAM Experience for Undergraduates"*. Teaching and Education Enhancement Program. Engineering Design and Rapid Prototyping. Massachusetts Institute of Technology.

[8] Gibson, I., Rosen, D., & Stucker, B. (2015). *Additive Manufacturing Technologies: 3D Printing, Rapid Prototyping, and Direct Digital Manufacturing*. Springer-Verlag, New York.

Journal of ENGINEERING in Medical Devices

DESIGN OF A MEDICAL DEVICE FOR SUPERFICIAL SUTURING UPPER AND LOWER EXTREMITIES

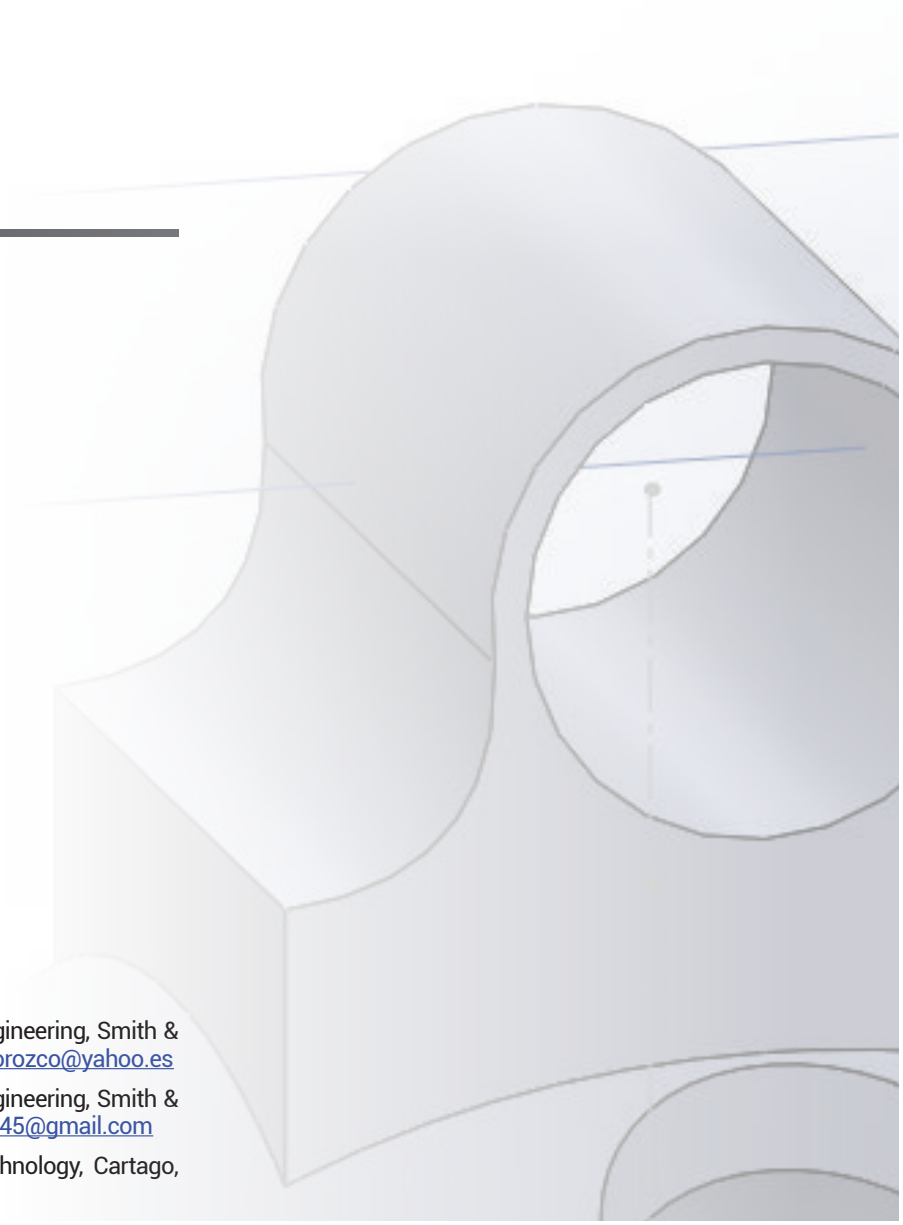

Michelle Orozco-Brenes[1]
José A. Jiménez-Chavarría[2]
Dagoberto Arias Aguilar[3]

Received: June 15th, 2017

Accepted: September 18th, 2017

[1] Engineer, Master in Medical Device Engineering, Smith & Nephew, Alajuela, Costa Rica, michelle.orozco@yahoo.es

[2] Engineer, Master in Medical Device Engineering, Smith & Nephew, Alajuela, Costa Rica, Joseaji1045@gmail.com

[3] Professor, Costa Rica Institute of Technology, Cartago, Costa Rica, darias@itcr.ac.cr

ABSTRACT

Suturing upper and lower extremities must be done quickly, evenly and easily. Therefore, the need to design a medical device that facilitates the health professional's work arises. This work presents the design for a class 2 medical device that meets the basic requirements of the current and known suturing methods in Costa Rica. The design process was achieved in three main stages, (i)Research on similar technologies; e.g. The operation principles of a sewing machine, materials used; (ii) The study of types of skin traumas; (iii) General approach toward the suturing device, including device functionality, integration with the human body and manufacturing process. The device model was designed and fabricated using 3D printing technology, this allowed the team to analyze ergonomics, the assembly of the parts and the equipment's motion. The printed prototype made it possible for potential users to provide feedback on the design and suggestions for improvement.

RESUMEN

La suturación de tejido humano en extremidades superiores con frecuencia requiere ser realizada de forma homogénea, sencilla y rápida. La necesidad de diseñar un dispositivo médico surge con el fin de facilitar la labor a los profesionales de la salud.

Este trabajo presenta el diseño de un dispositivo médico clase 2, capaz de suplir los requerimientos básicos de los métodos de sutura en Costa Rica. El diseño fue realizado en distintas etapas, (i) La investigación de tecnologías similares existentes; e.g, los principios de funcionamiento de una máquina de coser, materiales a utilizar en hilos y agujas; (ii) Reconocimiento de tipos de traumas en la piel; (iii) Planteamiento general del dispositivo de suturación, incluyendo funcionalidad del dispositivo, su integración con el cuerpo humano y su proceso de manufactura. El dispositivo fue modelado y fabricado por impresión 3D, con la intención de analizar su ergonomía, la integración de todas sus partes y el movimiento del equipo. La impresión del prototipo permitió a los usuarios potenciales dar su opinión respecto al diseño, y realizar sugerencias de modificaciones al mismo.

Keywords:

Suture, human tissue, 3D printing, medical device, 3D design software.

Palabras clave:

Sutura, tejido humano, impresión en 3D, dispositivo médico, diseño software 3D.

Journal of ENGINEERING in Medical Devices

Introduction

Skin plays a crucial role in protecting the human body and the health of an individual. It works as a barrier against the invasion of foreign substances and microorganisms, it helps regulate body core temperature, eliminates toxins and is the organ mainly in charge of receiving thermal and tactile stimulation [1]. However, frequently the skin suffers trauma easily resulting in open wounds.

The consequence of an open wound will usually be infection, attributable to environmental contaminants. Sutures are necessary when tissue is torn in such a way that natural healing is compromised. Left unsutured, skin takes a considerable period to join back together or will be completely unable to do so. The word "suture" describes the process of connecting blood vessels or drawing them near one and other by using a specific material [2]. When compared to other suturing techniques, suturing with thread provides the most resistant joint that will support the wound with minimal risk of dehiscence [3].

The idea for a medical device to suture arose for three main reasons. First, physicians were noticing poorly sutured wounds that would result in large scars. These in some cases required further procedures like plastic surgery. Also, time consumption, making the search for a device that would make the method faster a necessity. Finally, sutures stitched by hand are sometimes left too loose or too tight, causing bleeding from the wound. The visibility of the area is usually compromised, making the precision level of the procedure low and the variation between stiches substantial.

Suturing devices are internationally found in the market. However, they are not commonly used by hospitals in Costa Rica, mainly because they are expensive and complex. In summary, the objective of this work was to design a class 2 -FDA- electronic medical device, that minimizes tissue damage and is capable of quickly and uniformly suture a wound, leaving an aesthetically acceptable scar and allowing stitching to be simple and standardized.

Materials and Methods

The design searched for three main functions, (i) stabilize the skin, (ii) rotate the needle on its axis to join the tissue sections and (iii) initiate and finish with the least user interference possible. The result being a device that joins tissue quickly, avoiding any further hemorrhage or infection.

The application of computer assisted design (CAD) software SolidWorks® enabled the team to create a preliminary model design and check the specific movement capacity of each part, as shown in Figure 1. The height of the shell had to be redesigned while checking the movement on the software. The measurement of height had to permit the rotation of the needle on its axis without compromising the tissue against the device. The final design was oriented to have the area and volume of the shell as similar as possible for the needle to rotate 360° without any problem.

The design was 3D printed commercially to obtain a semi functional prototype. The parts for assembly were printed from STL files (Standard Tessellation Language). The first printer used was a Polyjet printer. This technology uses a liquid photopolymer that solidifies when exposed to an ultraviolet (UV) laser. The precision is considered high for this specific printer [4]. The piston was printed with this technology. The second printer used fused deposition modeling (FDM) technology, here the material is deposited from a nozzle were the material is added by layers. Layers can be modified by thickness and by a specific pattern [5]. Most of the parts were printed with this technology.

The use of a prototype allowed testing of certain functionality features before investing on an official model [6]. Figure 1 presents the 3D model that was used for the files printed.

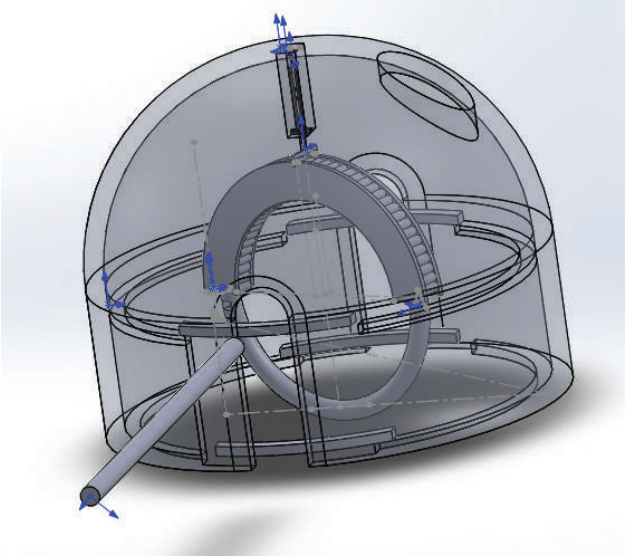

Figure 1. SolidWorks® design of the medical device to be printed.

The specifications of the model were as follows; functionality, cost, durability, modularity and reliability. The functionality looked for the suturing of upper and lower extremities with the least interference from the physician. The cost of generating the prototype was low due to the 3D printing technology used. The durability looked at lifespan. Materials have been contemplated for future production. The materials for a reusable medical device must be able to endure the sterilization process without compromising the device. The alloy AISI 316L was chosen for its resistance to fatigue and corrosion, its low friction coefficient, high strength and toughness [7]. The modularity will come in handy when re-loading the thread or switching needles. Finally, it's expected to work without problems or need of technical support covering reliability.

After the prototype was assembled and design functions checked, the final step required a survey. The prototype was presented to three Costa Rican physicians, (1) Dr. Stephanie Gómez Najéra, (2) Dr. Pamela Villareal Valverde and (3) Dr. Tatiana Piedra Chacón. The study contained questions about the medical device presented via prototype and they were asked to elaborate on their answers regarding their opinion as health professionals.

Results and Discussion

Table 1 presents the 6 main components of the suturing device. Each part is described briefly on its specific function. The type of threads this device was designed for are also shown in Table 1.

Table 1. Suturing medical device parts and functionality.

Part	Description
Shell	The device is held inside this part, its function is to work as main case for the device.
Guides	The guides allow the movement of the guide pin, it will fall in place by gravity. Each device has two guides.
Guide Pin	This pin is used to tie the knot. It is necessary that the device can perform a double knot.
Rollers	Main mechanism for the movement of the needle, the rotational movement that makes the suturing possible. It has two parts, the rollers and the restriction so the needle stays in place.
Piston	Provides the roles with the movement they require. Its parts are; Holder (holds roles), Pin (moves the holder in an axial fashion ±Y and 360°) and its Base that is fixed to the shell.
Needle	A ½ circle with tapered tip. Commonly used to suture.
Thread	For extremities gauges of 3/0 and 4/0, or thick gauges 1/0 and 2/0 are used. The material to be used is nylon, which is a polyamide obtained by chemical synthesis. Due to its elasticity, it is particularly useful for skin retention and closure [8].

Table 2 presents a step-by-step schematic representation on how the device works. The usage is simple, with the steps described as follows. (1) The

Journal of ENGINEERING in Medical Devices

needle is threaded while it is in its initial position, here the needle is out of the rollers and directed to the top of the shell. (2) The threaded needle is set in the rollers. (3) The piston is now in charge of lowering the shell. (4) The needle is rotated 270° pinching the tissue that will be sutured. (5) The rollers turn 45° to the right to initiate the knot while being guided by the holder. (6) The pin sets in place over the guide. (7) The needle turns 360° once more on its axis. (8) The guides now turn over the shell and release the guide pin, letting it fall due to gravity over the guides bellow, finishing what is the first knot. (9) The holder then takes the rollers to their initial position, (10) The holder turns 45° to the right again to start the second knot. (11) The needle rotates 360° on its axis. (12) The user will now tense the thread through the upper hole until the guide pin keeps it tense. (13) The lower guides will then release and the guide pin is removed. (14) The double knot is completed and the thread left should be cut with sterilized scissors.

The survey results are presented in Table 3. The numbers shown are the average between the three physicians that were part of the study. The scale used for the survey is based on the Likert scale. The scale goes for 1 to 5, specifically: strongly disagree, disagree, neutral, agree, strongly agrees, respectively.

The first question of the survey was met with both approval and disapproval. Two doctors said it would be useful time saving but only in simple suturing cases, the third doctor disagreed explaining that is a very simple procedure however, made a point that a person with very little training could suture with the device. The second question was met with similar responses, respectively to the use at their specific place of work. The comments referenced that the usefulness depends on the context of where it would be applied, for example a jail or emergency room. The following questions related to the design were well-received. One main drawback is that the device may not be suitable for all types of wounds. Other concerns raised by the physicians were related to the price and size of the device.

Table 2. Schematic representation of the function of the suturing medical device

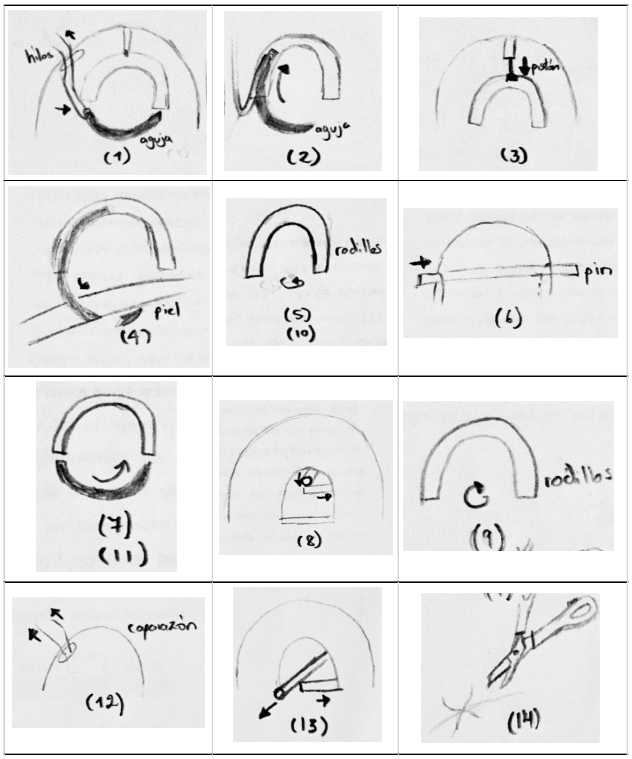

Table 3. Survey on trained medical physicians

Question	Item	Average
1	The device would be useful for myself	4
2	The device would be useful for my place of work	4
3	I would purchase a medical device like the one presented	4
4	The design is ergonomic	5
5	The device looks easy to use	5
6	The device resolved the need mentioned for suturing	5
7	The idea is original	5
8	The device can be used for different types of wounds.	3

Figure 2 shows the final design. The top figures show the 3D model and the bottom figures the final prototype, which was slightly modified to improve its ergonomic factor. The improvement was done at the top of the shell, and a holder was added to make it easier to manipulate and to add stability to the user. The change was made based on the observations obtained from the survey.

The prototype achieved its initial purpose. The next stage will be directed toward the mechanisms that will generate the movements of the device such as: motors, servomotor, sensors and electronic systems. The next step for the design would be the standardization of parts of the prototype allowing some specific pieces to be bought in the market instead of manufactured specifically for the device. The device is required to be transparent in some extend enabling an internal view of the affected area that is in need for suturing.

The end of this stage will allow the team to have a final model that meets the necessities described by the physicians in the survey. The manufacturing is expected to be simple allowing the device to reach the specific population it is designed for. The help of health professionals will continuously be needed during the process for guidance and recommendations.

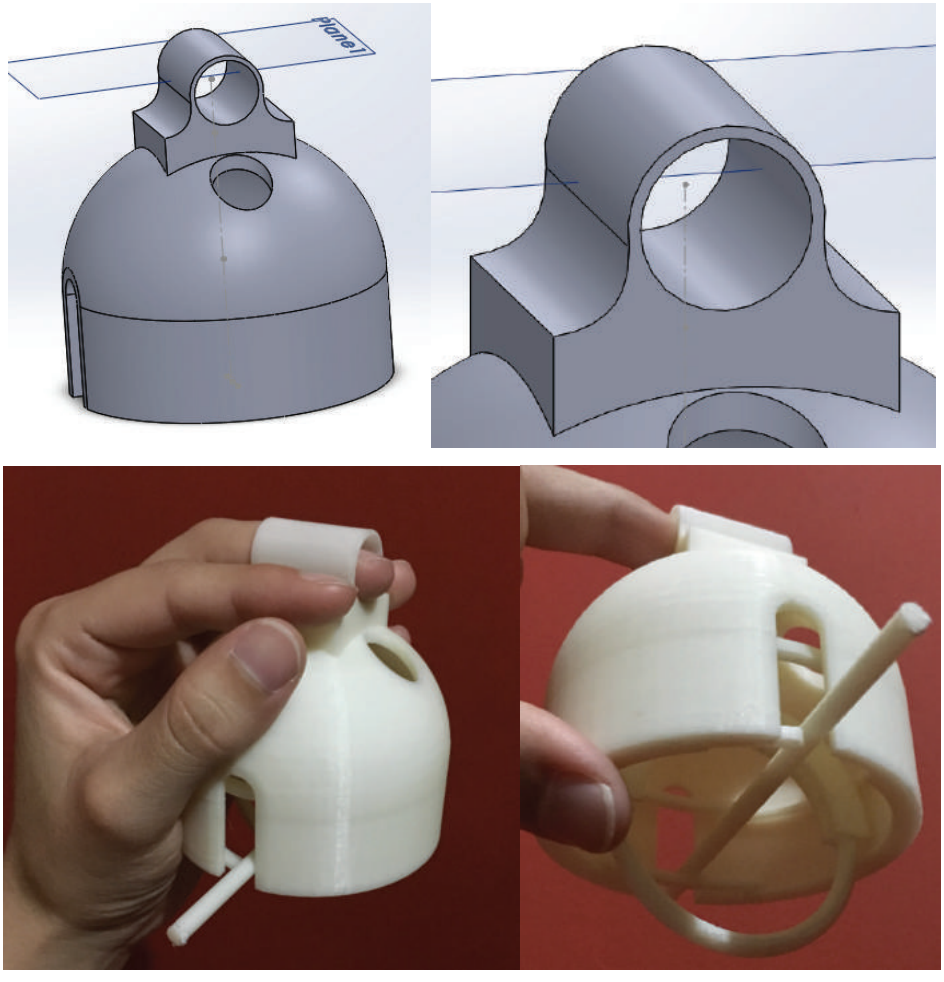

Figure 2. Final design for the suturing medical device

Journal of ENGINEERING in Medical Devices

Conclusions

1. The suturing device was accepted by the physicians during the development, and it would be useful for a lot of medical facilities. For the physicians, it is easy to use, and it needs a very low level of expertise.
2. The device adapts to wounds that requires suturing variations.
3. The idea is original and none of the doctors surveyed had seen anything similar.

Acknowledgements

The authors are grateful to Dr. Stephanie Gómez Najéra, Dr. Pamela Villareal Valverde and Dr. Tatiana Piedra Chacón for their participation in the survey, their collaboration with ideas and support for this study.

References

[1] Orozco-Razón, L.F., Milán-Guerrero, R.O., Vera-Rodríguez, S.E. (2002) Cianoacrilato comparado con cirugía tradicional en el cierre de heridas de zonas libres de tensión, *Gaceta Médica de México*, 138(6), 505-509.

[2] Hsiao, W.C., Young, K.C., Wang, S.T. and Lin, P.W. (2000) Incisional hernia after laparotomy: prospective randomized comparison between early-absorbable and late-absorbable suture materials, *World Journal of Surgery*, 24(6), 747-751.

[3] Arribas-Blanco, J.M., Castelló-Fortet, J.R., Rodríguez-Pata, N., Sánchez-Olaso, A., Marín-Guztke, M. (2002) Suturas básicas y avanzadas en cirugía menor (III), *Semergen*, 28, 89-100.

[4] The 3D Printing Solutions Company | Stratasys (2017). *Polyjet Technology*, Recovered from: www.stratasys.com

[5] Gibson, I., Rosen, D., & Stucker, B. (2015). *Additive Manufacturing Technologies: 3D Printing, Rapid Prototyping, and Direct Digital Manufacturing*. Springer-Verlag, New York.

[6] Weck, O., Wallace, P., Young, P., Yong Kim. *A Rewarding CAD / CAE / CAM Experience for Undergraduates*. Teaching and Education Enhancement Program. Engineering Design and Rapid Prototyping. Massachusetts Institute of Technology.

[7] ASM International (2005). *ASM Handbook, Volume 1, Properties and Selection: Irons, Steels, and High-Performance Alloys*. ASM International, Materials Park, OH.

[8] Oltra-Rodríguez, E., González-Aller, C., Mendiolagotia-Cortina, L., Sánchez-Quiroga, P. (2007) *Suturas y cirugía menor para profesionales de enfermería*, Madrid: Editorial Médica Panamericana.

Need finding activity in Costa Rican Hospitals

In order to define the topic for the graduation Projects, students go through a "need finding activity". Here in the photograph, Dr. Paul Fearis from John Hopkins University and Dr. Eric Richardson from Rice University are giving the lecture before the visit to Hospitals. Twenty-three students from the Costa Rica program and seven students from the Rice program visited several Costa Rican Public Hospitals to identify unmet needs.

Comments from the participating students about the activity:

- "Excellent global collaboration between TEC and RICE students along with the lecturing from both university professors, a winning formula".
- "Experience and guidance from international professors provided for a great learning experience".
- "Cutting edge strategies and a global focus of the medical device industry ".
- "Great opportunity for interaction in between students of both universities"
- "Collaboration in between TEC and RICE universities provided an exceptional environment for identifying needs at local hospitals".

New Anatomy and Physiology course

The Anatomy and Physiology class taught by Dr. Rodolfo Garbanzo Garvey, Research director at the Clínica Bíblica provides the students a unique hands-on experience during the laboratory sessions. As students work on designing medical devices, they need to understand the interaction in between the device and the human body.

The students provided feedback about the class:

- **"Laboratory sessions provided an insight that otherwise will not be possible"**
- **"Great course to understand the parts of the body and its functioning"**
- **"A course that integrates Engineering into the medicine field"**

Alternative Biomedical Materials for Prosthetics: Ti-6Al-7Nb and Nylon 6

Araya, Miguel[1],
Campabadal, Manuel[2],
González-Hernández, Joaquín[3]
Cubero-Sesin, Jorge M.[4]

Received: July 18th, 2017

Accepted: September 18th, 2017

[1] Professor, School of Industrial Design, Costa Rica Institute of Technology, Cartago, Costa Rica, miaraya@itcr.ac.cr

[2] Graduate student, Master Program in Medical Device Engineering, Costa Rica Institute of Technology, Cartago, Costa Rica.

[3] Professor, School of Materials Science and Engineering, Costa Rica Institute of Technology, Cartago, Costa Rica, jegonzalez@itcr.ac.cr

[4] Professor, Ph.D., Center for Research and Extension in Materials (CIEMTEC), School of Materials Science and Engineering, Costa Rica Institute of Technology, Cartago, Costa Rica, jcubero@itcr.ac.cr

Journal of ENGINEERING in Medical Devices

ABSTRACT

This research deals with the study and characterization of two materials with different chemical nature, a metallic alloy (Ti-6Al-7Nb) and an FDM 3D-printed thermoplastic polymer (Nylon 6), applying techniques such as metallographic analysis, scanning electron microscopy, energy dispersive spectroscopy and X-ray diffraction for the titanium alloy; and Fourier transform infrared spectroscopy and differential scanning calorimetry for the analysis of the Nylon polymer. Among the most relevant results for the titanium alloy stands the presence of two phases in the crystal structure: a primary phase α immersed in a duplex matrix (α+β), with a lower fraction of β crystals. The X-ray analysis showed the existence of Ti and TiO in the sample. For the polymeric sample, it was possible to identify the basic structure with infrared analysis, confirming that the sample is from a Nylon 6 filament. Also, the calorimetric analysis made possible the identification and comparison of the melting temperature for both raw and processed samples.

RESUMEN

Esta investigación trata con el estudio y caracterización de dos materiales con diferente naturaleza química, una aleación metálica (Ti-6Al-7Nb) y un polímero termoplástico impreso en 3D por FDM (Nylon 6), aplicando técnicas como análisis metalográfico, microscopía electrónica de barrido, espectroscopía de energía dispersiva y difracción de rayos-X para la aleación de titanio; y espectroscopía infrarroja por transformada de Fourier y calorimetría diferencial de barrido para el análisis del polímero Nylon. Entre los resultados más relevantes para la aleación de titanio alloy, se encuentra la presencia de dos fases en la estructura cristalina: una fase primaria α inmersa en una matriz duplex (α+β), con una fracción menor de cristales de β. El análisis de rayos-X mostró la existencia de Ti y TiO en la muestra. Para la muestra polimérica, fue posible identificar la estructura básica con el análisis infrarrojo, confirmando que la muestra proviene de un filamento de Nylon 6. Adicionalmente, el análisis calorimétrico hizo posible la identificación y comparación de la temperatura de fusión tanto para la muestra virgen como para la procesada.

Keywords:

Titanium alloy, Nylon, Characterization, SEM, XRD, FTIR, DSC.

Palabras clave:

Aleación de Titanio, Nylon, caracterización, SEM, XRD, FTIR, DSC.

1. Introduction

Ti-6Al-7Nb is a relatively new titanium alloy. The mechanical properties of Ti-6Al-7Nb alloy are very similar to Ti-6Al-4V alloy, which has been used as a biomaterial for many years. The major difference between the alloys is the replacement of Vanadium with Niobium [1]. This is because Vanadium is released as cytotoxic ions with time, while Niobium ions do not exhibit this behavior, and in turn are considered as vital for cellular functions [2].

Based on the phase analysis by metallography, scanning electron microscopy (SEM) coupled with energy dispersive spectroscopy (EDS) and other material characterization techniques such as X-ray diffraction (XRD), it is possible to to identify structures and crystalline compounds in metallic alloys [3].

In addition, ASTM E 92-82 standard [4] defines the Vickers microhardness test as an indentation method, in which, by the use of a calibrated machine with a pyramidal square based indenter, a predetermined load is applied against the material test surface. The measure of the resulting size of the indentation after removing the load, is proportional to the resistance of the material to plastic deformation. The Vickers microhardness test can provide a correlation of the atomic structure with the mechanical properties [4].

The polyamides were the first engineering thermoplastics produced specifically by design as a plastic, and are the largest family in both production volume and number of applications [5].

Fused Deposition Modeling (FDM) 3D printing technology has been used for prototyping and end-use products and parts, applying high performance thermoplastics [6]. Nylon is one of most used polymers for FDM technology, presenting a low cost custom design alternative. Materials characterization techniques such as Fourier transform infrared (FTIR) spectroscopy and differential scanning calorimetry (DSC) can be performed to detect if the thermoplastic polymer properties are affected by temperature during 3D printing.

The purpose of this study is to document the characterization of new materials that could be used to manufacture prosthetics by additive manufacturing techniques, in order to aid in creating design criteria to make process optimization decisions in the future application of these technologies.

2. Experimental Procedure

The characterization study of titanium alloy Ti-6Al-7Nb and the polymer Nylon 6 were performed by different techniques. The diagram in Fig. 1 shows the experimental strategy of this study.

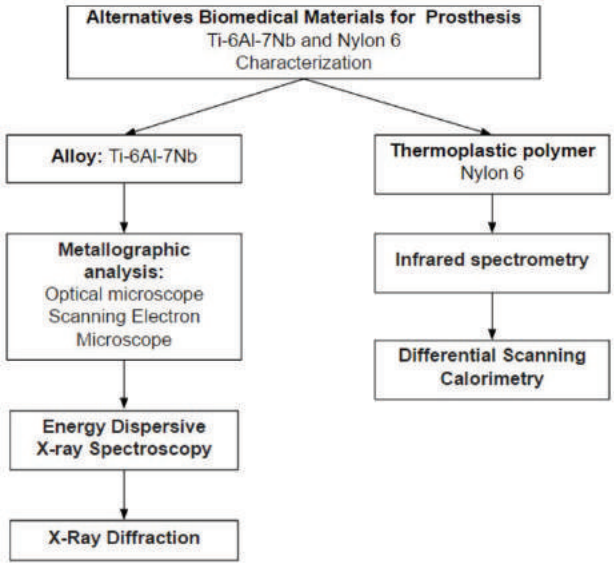

Fig.1. Experimental Strategy.

2.1 Metallic alloy sample: Ti-6Al-7Nb

The sample preparation for the metallographic analysis was performed at the Center for Materials Research and Extension (CIEMTEC, School of Materials Science and Engineering, Costa Rica Institute of Technology). Samples were mounted on thermoplastic resin and polished using SiC paper. Buffing was carried out with 1 µm particle size alumina suspension to a mirror-like surface, and finally chemical etching was performed to reveal microstructures for observation under the optical microscope. The chemical solution for etching was: 11% $HF_{(ac)}$, 59% $C_3H_6O_{3(ac)}$, 24.6% $H_2SO_{4(ac)}$, 3.6% $C_2H_6OS_{(ac)}$ and 1.8% $C_3H_8O_3$.

A Mitutoyo HM-101 hardness tester located in the Center for Materials Research and Extension (CIEMTEC, School of Materials Science and Engi-

Journal of ENGINEERING in Medical Devices

neering, Costa Rica Institute of Technology) was used to measure the Vickers microhardness. The load of 200 g was applied for 15 s. A total of 10 measurements were carried out on the surface of the as-polished sample.

The grain size and phase characteristics of the alloy were also analyzed in a Hitachi TM-1000 scanning electron microscope (Institutional Microscopy Laboratory, Costa Rica Institute of Technology). The SEM was operated with an electron acceleration voltage of 15 KV. Also, the EDS spectrometer was used to analyze the concentration of the elements present in the alloy. The XRD analysis was performed with the PANalytical Empyrean X-ray diffractometer located in the Center for Materials Research and Extension (CIEMTEC, School of Materials Science and Engineering, Costa Rica Institute of Technology). A copper target with $\lambda = 1.54$ Å $K\alpha_1$ radiation was used, using a voltage of 45.0 KV and current of 40.0 mA. A divergence slit of ½° and anti-scatter slit of 1° were used, respectively. The sample was scanned with the goniometer range of $2\theta = 30^{o}$-80^{o}.

2.2 Thermoplastic polymer sample: Nylon 6

For the FTIR spectroscopy, a section of Nylon filament was cut and placed in the ATR holder of a Nicolet 6700 FTIR spectrometer located at the National Nanotechnology Laboratory (LANOTEC-CeNAT). HR Hummel Polymer and Additives Library was used to identify the polymer structure.

The thermal analysis was performed with the DSC equipment TA Q200 located at the National Nanotechnology Laboratory (LANOTEC-CeNAT), with a heat only calibration method, on a range from 100 to 250 °C. The temperature accuracy was of ± 0.1 °C. The initial sample weight was 4.5 mg with air as the sample reference. The samples for the DSC analysis were extracted from a Nylon filament (raw material) and from a 3D printed part with the same material (processed material).

3. Results and Discussion

3.1 Ti-6Al-7Nb

Optical Microscopy and SEM

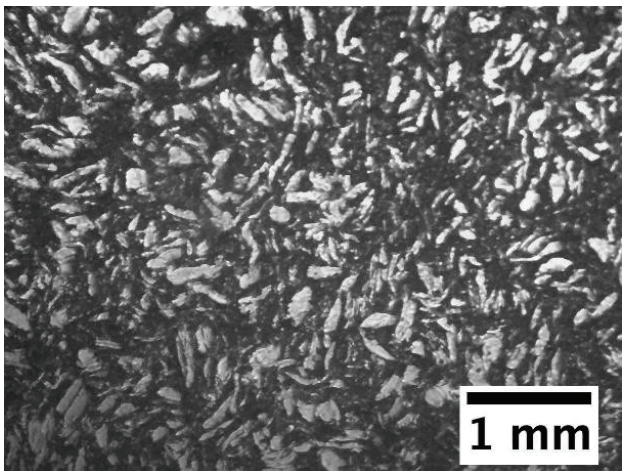

Fig. 2. Metallography of Ti-6Al-7Nb: Optical Micrograph 400x.

Fig. 2 shows the microstructure of Ti-6Al-7Nb; which reveals the presence of two phases. As it is known, the duplex type structure (α+β) is characteristic for this alloy composition [1]. The dark contrast corresponds to an α+β matrix and the bright grains correspond to the primary alpha phase (α). The α phase has a hexagonal close-packed crystal structure (HCP), while the β phase exhibits a crystalline arrangement in the body centered cubic (BCC) structure [7].

Fig. 3 shows a SEM image from a region within the one shown in Fig. 2. It shows the matrix phases (α+β) in higher magnification, with the β particles in bright contrast, surrounding the α component of the matrix. The primary α grains have darker contrast but with different hues (some darker than others), this is due to the different orientations of the crystals. These areas are rich in aluminum (Al), because the Al stabilizes the alpha phase. Additionally, the grains of the β phase which are immersed in the matrix are rich in niobium (Nb) because Nb stabilizes the beta phase [7].

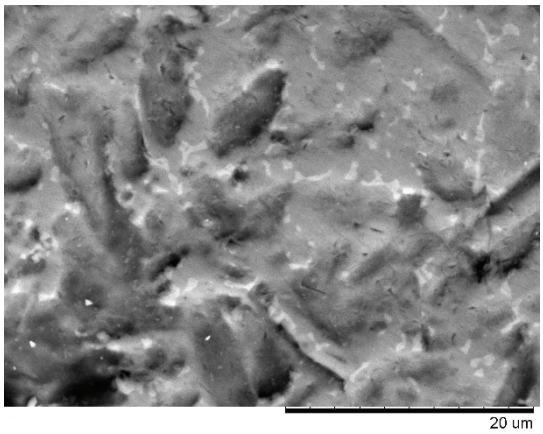

Fig. 3. Metallography of Ti-6Al-7Nb: SEM image 4000x.

Energy Dispersive Spectroscopy analysis

EDS was used to determine the chemical composition from the phases shown in the image of Fig. 3. The results in Fig. 4 show that two characteristic elements (Ti and Al) from the alloy Ti-6Al-7Nb were detected. The larger mass percentage corresponds to Ti since it is the main component. However, since EDS detects the chemical composition in the near surface, some other elements were detected, mainly C and O, and are included in the calculation of the total fraction. Thus, the fraction of Ti is much lower than expected. Nonetheless the ratio of Al to Ti is consistent with the alloy composition. C is detected from the conductive tape that holds the sample in the instrument, as well as from surface contamination, so it can be neglected from the composition of the alloy itself.

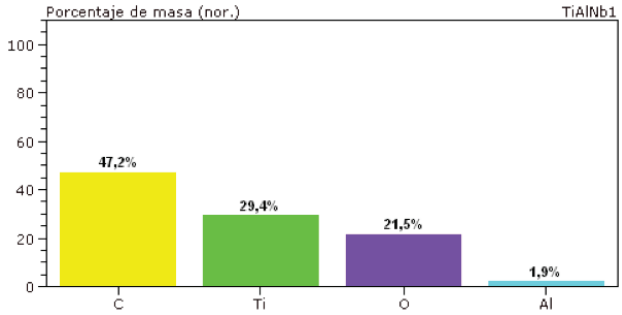

Fig. 4. Chemical composition of Ti-6Al-7Nb (mass percentage) obtained from EDS analysis

In the case of O, the high fraction is possibly due to the titanium oxides than are generated in the surface, which gives Ti its high corrosion resistance, as it acts as a passivation layer [7]. Since Nb is only present in the fine β phase, it was difficult to detect by EDS due to the small size of the particles, as shown in Fig. 3.

XRD analysis

The diffraction pattern of the Ti-6Al-7Nb sample shown in Fig. 5 confirmed the presence of the hexagonal compact crystalline structure of α-Ti phase, which has three main peaks (in order of intensity) at 2θ = 40.416° (101 plane) 2θ = 38.439° (002 plane) and 2θ = 63.204 ° (110 plane). All other peaks corresponding to α-Ti are shown in Fig. 5 with their respective Miller indices 2θ = 35.308° (100), 2θ = 53.212° (102), 2θ = 70.785° (103), 2θ = 76.084° (112). As mentioned in the previous section, Ti-6Al-7Nb presents two phases (α+β); however, the diffraction pattern corresponding to the β peaks overlap with the peaks of the α phase, so it cannot be isolated by XRD. The positions corresponding to the β phase are indicated in Fig. 5. In addition, characteristic diffraction peaks of titanium oxide (TiO), with monoclinic crystal structure were detected, with the three main peaks in order of intensity 2θ = 42.694° (121), 2θ = 40.486° (400) and 2θ = 63.464° (511). TiO presence was expected because the passivation layer is present in the surface of the sample, and is consistent with the high O content detected by EDS.

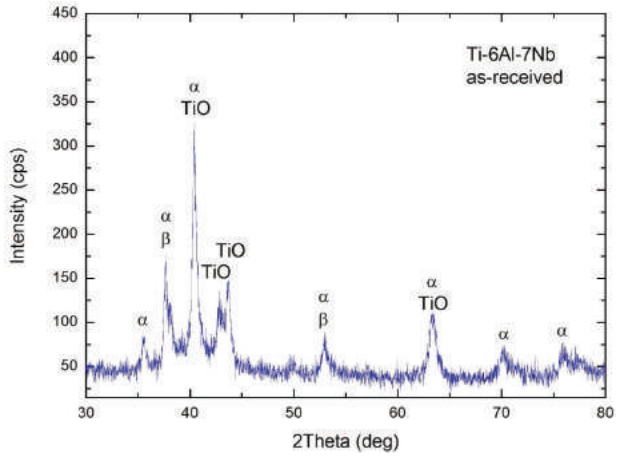

Fig. 5. Ti-6Al-7Nb XRD profile

Vickers Hardness Test

Table 1 shows results of the microhardness measurements carried out in different regions of the sample. The average hardness value is ~292 HV,

Journal of ENGINEERING in Medical Devices

which is consistent with the reported value in the literature of 270-290 HV for the wrought Ti-6Al-7Nb [7]. Additionally, variations in the magnitudes of microhardness are observed, which accounts for a standard deviation of ~10 HV. This is due to the presence of two phases, whereby, some indentations include higher proportion of either primary or (α+β) phase.

Table 1. Vickers microhardness measurements of Ti-6Al-7Nb

Measurement	HV (±0.1)
1	297.6
2	296.0
3	286.2
4	283.0
5	287.8
6	306.2
7	279.9
8	299.3
9	304.5
10	279.9
Average	292.04
Standard deviation	9.91

3.2 Nylon 6

FTIR Spectroscopy

The FTIR spectroscopy analysis allowed to identify the basic structures present in the chemical configuration of Nylon 6, and to carry out a correlation with the structures of the HR Hummel Polymer and Additives database. The FTIR spectrum of the sample analyzed is represented in Fig. 7, and the similarity correlation is shown in Fig. 8. The vibrational frequencies represented in the spectrometry result, gave information to confirm the basic molecular structure of Nylon 6, and therefore confirm the polymer provided by the supplier of the filament. Characteristic bands of C (O) NH appear around 3296, 1634 and 1540 cm^{-1} in the spectrum [8].

Table 2 shows the results of the similarity correlation of the infrared spectrum obtained from the Nylon sample. Comparison with the HR Hummel Polymer and Additives Library, confirmed that the supplier of the filament possibly provides Nylon 6, with 72.47% of similarity with the polymer Poly(amide 6,6:amide 6) from the database. Other results with similar correlation indices all correlate to commercial or ideal structures of Nylon 6 or Nylon 6,6.

Differential Scanning Calorimeter DSC

A sample was analyzed before and after an FDM 3D printing in order to compare how the melting process affected its thermal properties. The DSC curve comparison between the raw sample and the processed sample is shown in Fig. 9. The results show that the composition of the sample probably was not affected, since the response of the material is very similar when it is heated to the melting temperature. The melting temperature (T_m), is ~196 °C for the raw filament, which is important to characterize the optimal process specifications for FDM 3D printing. In terms of the FDM process parameters provided by the supplier of the filament, the material should be heated up to 220 °C, and has a consistent material flow at 275 °C, so it is clear the process is well within specification. Fig. 9 also shows there is a slight increase in the T_m to ~202 °C after the process, possibly due to thermal memory imprinted by the FDM process.

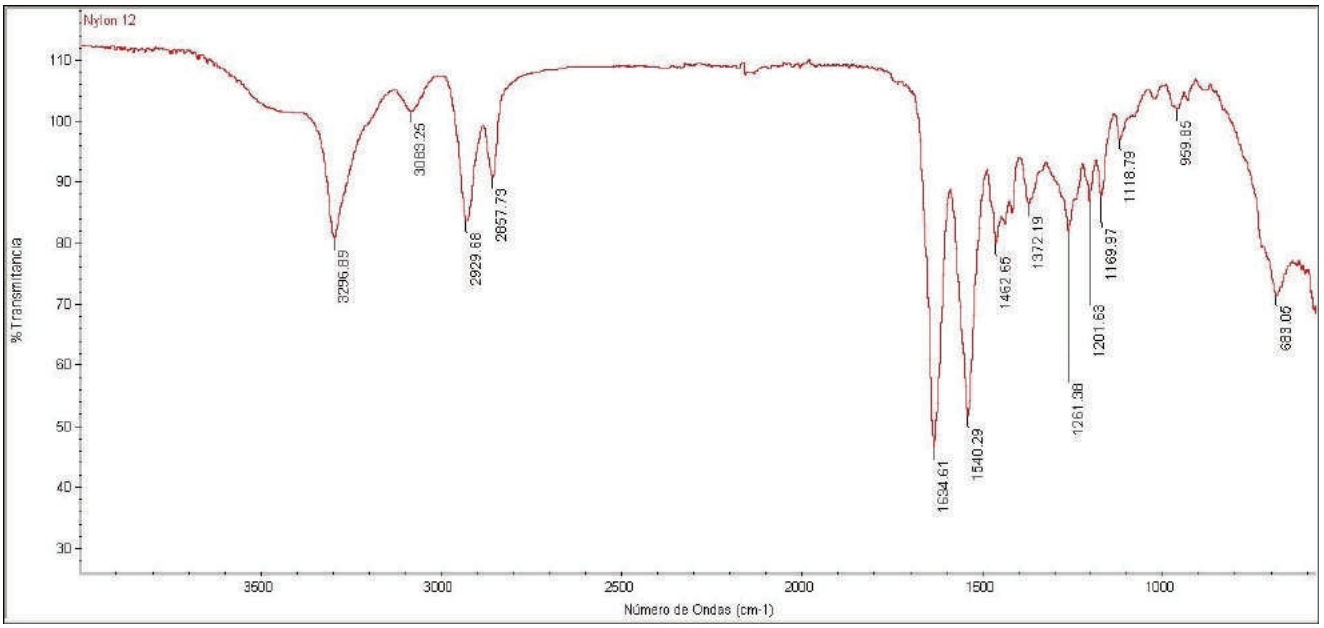

Fig. 7. FTIR spectrum obtained from the Nylon sample.

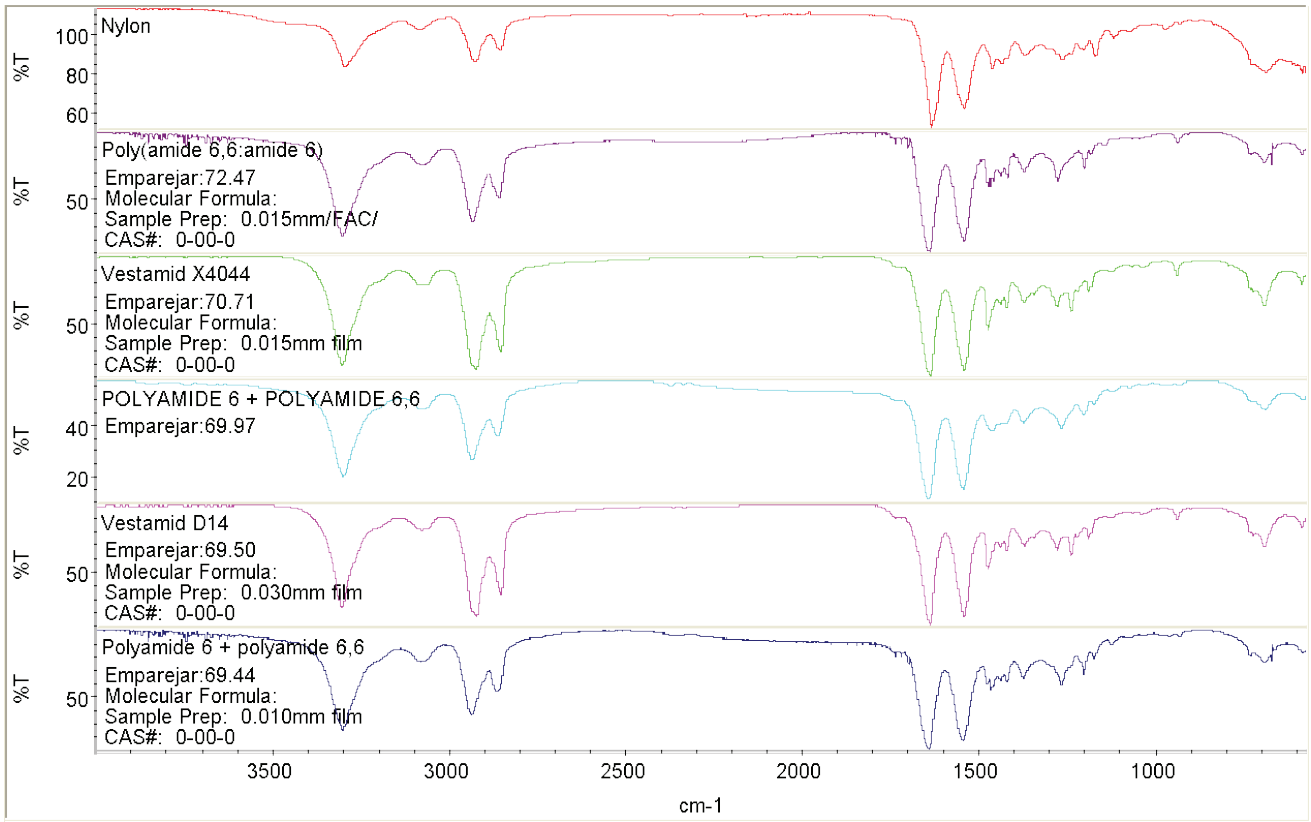

Fig. 8. Similarity correlations of FTIR spectrum obtained for Nylon sample with the HR Hummel Polymer and Additives library.

Journal of ENGINEERING in Medical Devices

Table 2. Similarity correlation of FTIR spectrum obtained for Nylon sample.

Index	Similarity %	Compound Name	Library
290	72.47	Poly(amide 6,6:amide 6)	HR Hummel Polymer and Additives
1025	70.71	Vestamid X4044	HR Hummel Polymer and Additives
28	69.97	POLYAMIDE 6 + POLYAMIDE 6,6	HR Hummel Polymer and Additives
1024	69.50	Vestamid D14	HR Hummel Polymer and Additives
286	69.44	Polyamide 6 + polyamide 6,6	HR Hummel Polymer and Additives

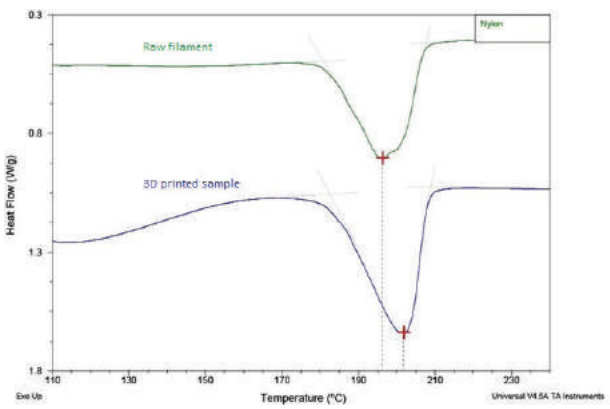

Fig. 9. Nylon 6 DSC curves before and after 3D printing.

4. Conclusions

The metallographic analyses provided information about the microstructures in the Ti-6Al-7Nb alloy. Two phases were identified: an α primary phase with grains immersed in an α+β matrix. SEM was used to identify the morphology of the β phase in the matrix, as fine particles with a low fraction with respect to α phase.

By the EDS analysis high concentration of Ti and O were detected, which corresponds to the passivation layer of the Ti-6Al-7Nb alloy. Al, but not Nb, was detected since it is present in the α phase, which has a larger fraction with respect to β, which is rich in Nb.

From the XRD analysis of Ti-6Al-7Nb, Ti (HCP) structure corresponding to the α phase, and TiO (monoclinic) structure corresponding to the passivation layer of the alloy, were identified as the main crystal structures. The characteristic peaks of β phase overlapped with the peaks of the α phase.

Using FTIR analysis it was possible to identify the polymer as Nylon 6, confirming that it has a Polyamide 6 basic molecular structure. This information was useful in a subsequent DSC analysis, in which it was possible to compare the melting point of the sample before and after an FDM manufacturing technology, and also to compare it with the specifications provided by the supplier of the filament.

Acknowledgements

The authors are grateful to Felipe Orozco from the National Nanotechnology Laboratory (LANOTEC-CeNAT), to Esteban Rodríguez from the Center for Research and Extension in Materials (CIEMTEC) of the Costa Rica Institute of Technology, and to Luis Alvarado Marchena from the Institutional Microscopy Laboratory of the Costa Rica Institute of Technology, for their assistance and guidance in carrying out the analyses.

5. References

[1] Janecek, M., Stráský, J., Cizek, J., Harcuba, P., Vaclavoá, K., Polyakova, V., Semenova, I., (2014). Ultrafine-grained biocompatible Ti-6Al-7Nb alloy was produced by high pressure torsion. *Metallurgical and Materials Transactions A*. 45, 7-15.

[2] Oshida, Y. (2007). *Bioscience and Bioengineering of Titanium Materials*. Elsevier, Great Britain, 1st ed.

[3] Cullity, B., Stock, S. (2001). *Elements of X-Ray Diffraction*. United States of America: Prentice Hall. 3rd ed.

[4] American Society for Testing and Materials. *Standard Test Method for Vickers Hardness of Metallic Materials*. ASTM E 92-82/

[5] Charles, J., Ramkumaar, G.R., Azhagiri, S., Gunasekaran, S., (2009) FTIR and Thermal Studies on Nylon-66 and 30% Glass Fibre Reinforced Nylon-66. *Journal of Chemistry*, 6(1), 23-33.

[6] Matsuzaki, R., Ueda, M., Namiki, M., Jeong, T.K., Asahara, H., Horiguchi, K., Nakamura, T., Todoroki, A., Hirano, Y. (2016) Three-dimensional printing of continuous-fiber composites by in-nozzle impregnation. *Scientific Reports*, 6, 23058.

[7] Geetha, M., Singh, A. K., Asokamani, R., Gogia, A. K. (2009) Ti based biomaterials, the ultimate choice for orthopaedic implants—a review, *Progress in Materials Science*, 54(3), 397–425.

[8] Chonde Sonal, G., Chonde Sachin, G., Raut P.D. (2013). Studies on degradation of synthetic polymer Nylon 6 and Nylon 6,6 by Pseudomonas aeruginosa NCIM 2242. International Journal of Emerging Technologies in Computational and Applied Sciences, 4(4), 362-369.

Journal of ENGINEERING in Medical Devices

CHARACTERIZATION OF ETHYLENE-VINYL ACETATE (EVA) USED IN ORTHOPEDIC INSOLES

Miguel Ángel Zerpa-Catanho[1], Ana Julia Sanahuja-Vindas[2], Sebastián Cordero-Hidalgo[3], Adrián Bogantes-Saborio[4], Jorge Cubero-Sesin[5]

Received: June 15th, 2017

Accepted: September 18th, 2017

1. Industrial Design Engineer, ErgoTEC - Applied Ergonomic Laboratory, Costa Rica Institute of Technology, mazc21@gmail.com
2. Microbiologist, Abbott, Costa Rica, ana_05sanahuja@hotmail.com
3. Industrial Design Engineer, Mckinsey & Company, America Free Zone, Costa Rica, sebascordero@gmail.com
4. Physiotherapist, Fisiosport, Costa Rica, adrianbogantestf@gmail.com
5. Professor, Ph.D., Center for Research and Extension in Materials (CIEMTEC), School of Materials Science and Engineering, Costa Rica Institute of Technology, Cartago, Costa Rica, jcubero@itcr.ac.cr

RESUMEN

Las órtesis son parte de la inmensa industria de dispositivos médicos cuyo objetivo es mejorar la vida del paciente, mediante la corrección o el tratamiento de lesiones. Por lo tanto, es de gran importancia comprender las propiedades físicas, químicas y mecánicas de los materiales utilizados para desarrollar estos productos. Esta investigación utiliza las técnicas de difracción de rayos-X, análisis de termogravimetría y calorimetría diferencial de barrido, espectroscopía infrarroja por transformada de Fourier y microscopía electrónica de barrido, para la caracterización del etilvinilacetato (EVA) utilizado en Costa Rica para la fabricación de plantillas ortopédicas. Dichas técnicas permitieron identificar características específicas de dos muestras de EVA con distinto valor de dureza en la escala Shore, tales como la presencia de carbonato de calcio ($CaCO_3$), la cantidad de acetato de vinilo presente en el compuesto, una temperatura de fusión de 72° C y diferencias en la densidad del material. Los resultados mostraron que la razón principal en la variación de dureza entre ambas muestras es la cantidad de acetato de vinilo presente, la cual se puede aumentar o disminuir según requisitos específicos.

ABSTRACT

Orthotics are part of the immense medical devices industry; their aim is to improve the patient's life by correcting or treating injuries. Therefore, it is of great importance to understand the physical, chemical and mechanical properties of the materials used to develop these products. This research uses techniques such as X-ray diffraction, thermogravimetric and differential scanning calorimetry analyses, Fourier transform infrared spectroscopy and scanning electron microscopy, for the characterization of ethylene-vinyl acetate (EVA) used for manufacturing orthopedic insoles in Costa Rica. These techniques allowed to identify specific characteristics of two EVA samples with different value of hardness in the Shore scale, such as the presence of calcium carbonate ($CaCO_3$), the amount of vinyl acetate in the compound, a melting temperature of 72° C, and differences between the material's densities. The results show that the main reason in the variation of hardness between both samples is the amount of vinyl acetate present which can be increased or reduced according to specific requirements.

PALABRAS CLAVE

Acetato de etileno-vinilo, acetato de vinilo, ortopedia, dispositivo médico, plantillas ortopédicas.

KEYWORDS

Ethylene-vinyl acetate, vinyl acetate, orthotics, medical device, orthopedic insoles.

Journal of ENGINEERING in Medical Devices

INTRODUCTION

Feet are structures subject to high levels of biomechanical stress and impact due to their overuse in activities of daily life or sports; therefore, the presence of dysfunctions in musculoskeletal or neuronal structures are common; this stress and impact can cause pain and even disability [1,2].

The use of orthotics as means of correction and treatment of injuries caused by abnormal structures or foot joint dysfunction is a common practice. This orthotics must resist abnormal foot pressure; aiming to correct and restore normal alignment of the lower extremities, in order to promote proper foot support on uneven and unstable surfaces [3].

Currently, there are different hardness levels for this polymer (according to the Shore hardness scale) used in the manufacturing processes of these medical devices. Hardness level are personalized depending on the clinical needs of the patient; therefore, it is of great interest to determine what compounds in the molecular structure of the material modify the polymer properties by increasing or decreasing its hardness.

This study allowed to characterize Ethylene-Vinyl Acetate (EVA) using different methods. X-ray diffraction (XRD) has its origin in the elastic dispersion of the X-ray beam that passes through the atoms of the sample, where the electrons of the material disperse the wave at the same angle of incidence (θ-Theta), hence this radiation emerges at an angle 2θ with respect to the direction of the incident beam, conserving its initial energy. This type of diffraction is described by the Bragg Law which predicts in what direction a constructive interference occurs between the electromagnetic waves dispersed in a crystal [4].

Thermogravimetric Analysis (TGA) is a method of thermal examination where changes in the chemical and physical properties of the material are measured in relation to changes in temperature (or isothermal as a function of time). This information allows the study of phenomena such as: decomposition of the material, phase transitions, desolvation and solid-gas reactions. It is possible to detect such reactions if there is change in mass related to the change in temperature [5]. Differential scanning calorimetry (DSC) is another thermoanalytical technique where the heat difference needed to increase the sample temperature and that of a reference material is measured as a function of temperature [6].

Fourier Transform Infrared spectroscopy (FTIR) is a vibrational spectroscopic technique used to obtain a spectrum on a large variety of simultaneous wave elements, creating a spectrum that collects separate signals at each wave number [5]. This thermal energy radiation (low-energy electromagnetic waves) induces molecular vibrations in covalent bonds, which can vibrate in different ways, including symmetrical and asymmetrical stretching, swinging, scissor, flutter and twist vibrations. This technique can provide information about the functional groups of an unknown molecule. It is a widely-used method for performing measurements, quality control and dynamic measurements. It also allows to measure the degree of polymerization in the manufacturing of polymers [5].

Scanning Electron Microscopy (SEM) analysis, is a technique in which images are produced from a sample that is scanned by a focused beam of electrons. These electrons interact with the atoms of the sample producing secondary and backscattered electrons, as well as characteristic X-rays, which are quantified by different detectors and produce information about the topology and chemical composition of the sample [5].

The main limitations of the study revolve around the difficulty of performing repetitive tests on the polymer samples, so the results obtained are unique and are not comparable with other results from the same sample. It is understood that EVA is a composite polymer but the molecular structure and chemical composition is unknown, making it difficult to relate the results obtained with the production sheet of the material where it was synthesized.

Understanding the physical, chemical and mechanical properties of the material used for the

construction of 3D printed insoles is essential to ensure success in therapy. Through the analysis of elemental composition in the molecular structure, this work intends to characterize the EVA material, which is used for manufacturing orthopedic insoles in Costa Rica, by means of the aforementioned techniques.

MATERIALS AND METHODS

X-Ray Diffraction Analysis (XRD)

In order to obtain the chemical compounds or phases present in the crystalline structure of EVA polymer, an X-ray diffraction analysis was conducted. The samples were pulverized EVA material of 50 shore hardness (EVA 1) and pulverized EVA of 25 shore hardness (EVA 2), with a PANalytical Empyrean diffractometer, located at the School of Materials Science and Engineering, Costa Rica Institute of Technology. This diffractometer used a radiation source of copper (Cu-K_{α}) powered with 40 mA and 45 KV. The analysis was carried out at room temperature with a scanning range from 10° to 80° (2θ), step size of 0.0130° (2θ) and a scan step time of 3.57 s.

Thermogravimetric Analysis (TGA)

This test was performed at the National Nanotechnology Laboratory (LANOTEC-CeNAT) with the TGA Q500 from TA Instruments, under at ultra-high-purity nitrogen atmosphere, with a balance gas of 10.0 ml/min and sample gas of 90.0 ml/min. The temperature ramp used in this technique was at 20° C/min from 30° C to 500° C, at this point, the ramp was increased to 50° C/min up to 1000° C. The air cool time was 25.0 min.

Differential Scanning Calorimetry (DSC)

The experiment was performed at the National Nanotechnology Laboratory (LANOTEC-CeNAT), using the DSC Q200 from TA Instruments. It was possible to obtain information about the purity of the EVA samples, transitions of state (fusion and glass transition, among others), and the effect of stabilizers and pressure [5]. The temperature range used for this analysis was from 25° C to 150° C, with a 20° C/min ramp in an inert atmosphere of ultra-high-purity nitrogen (50.0 ml/min). This atmosphere was also used as a reference material during the experiment.

Fourier Transform Infrared Spectroscopy (FT-IR)

The ThermoScientific Nicolet 6700 FT-IR with the ATR (Attenuated Total Reflectance) sampling accessory, located at the National Nanotechnology Laboratory (LANOTEC-CeNAT), was used on a small sample of the material pressed on top of the diamond crystal. A total of 32 scans were averaged, provided the necessary information for this analysis from the pattern library in the equipment.

Scanning Electron Microscopy (SEM)

This test was performed at the Institutional Microscopy Laboratory, Costa Rica Institute of Technology, using a HITACHI TM-1000 microscope. A Denton Vacuum Desk IV ion coater was used to coat the sample in a gold-palladium conductive layer to allow the conductance of electrons in the surface, given that EVA is not conducting material.

RESULTS

XRD Analysis

Table 1 and 2 show the results of XRD analysis for peaks of the EVA 1 and EVA 2 samples, respectively. The tables show the position angle, peak height, peak width at half maximum (FWHM), atomic d-spacing and the relative intensity of each sample peak. Analysis of the EVA 1 and EVA 2 samples by XRD allowed the indexation of their diffraction spectra, with a match to Ethylene-Vinyl Acetate polymer spectrum of the equipment data library, as shown in Figure 1. The most significant difference between the spectra corresponds to the position of the highest intensity peak, where for EVA 1 it is in the crystallographic plane (100) (2θ=21.3980°) and

Journal of ENGINEERING in Medical Devices

for EVA 2 in (210) (2θ=29.5299°). Table 3 shows the positions (2θ) of the Ethylene-Vinyl Acetate polymer spectrum, its interplanar distances and the respective Miller Indices. There was also a match for calcium carbonate ($CaCO_3$) in both samples. The peaks for this substance are close to the EVA reflections at 29.3905°, 39.3997° and 48.4891°, corresponding to the (104), (113) and (116) planes.

Table 1. *Results of the EVA 1 XRD analysis.*

POS. (°2 Th.)	HEIGHT (cts)	FWHM LEFT (°2 Th.)	D-SPACING (Å)	REL. INT. (%)
21. 3980	1192.67	0.3838	4.15264	100.00
23.5461	227.43	0.3070	3.77844	19.07
26.5812	58.13	0.2047	3.35350	4.87
29.4120	830.26	0.2558	3.03687	69.61
31.4852	26.81	0.4093	2.84147	2.25

Table 2. *Results of the EVA 2 XRD analysis.*

POS. (°2 Th.)	HEIGHT (cts)	FWHM LEFT (°2 Th.)	D-SPACING (Å)	REL. INT. (%)
21.4520	150.33	0.5117	4.14232	45.65
23.2129	51.14	08187	3.83191	15.53
27.5578	44.67	0.2047	3.23684	13.56
29.5299	329.32	0.1791	3.02501	100.00
36.2522	74.76	0.3070	2.47803	22.70

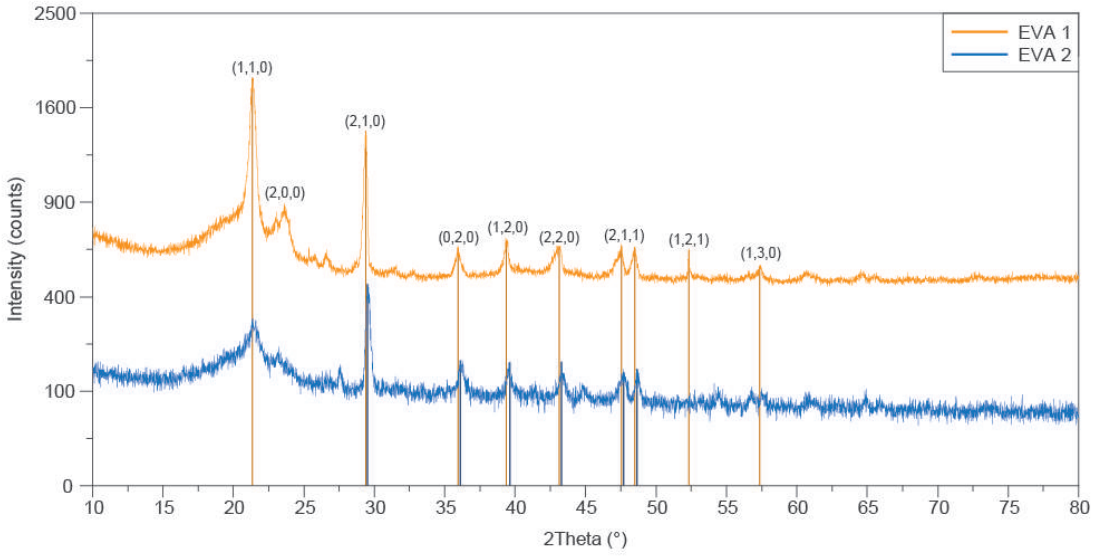

Figure 1. *Comparative XRD graph of EVA samples.*

Table 3. X-Ray Diffractometry Reference for EVA Polymer.

POS. (°2 Th.)	D-SPACING (Å)	I	h	k	l
21.4826	4.132970	999	1	1	0
23.7245	3.747230	197	2	0	0
29.8714	2.988650	9	2	1	0
36.2333	2.477160	36	0	2	0
38.2342	2.352000	14	1	2	0

TG Analysis

Figure 2 shows the comparative chart of the TG analyses corresponding to the EVA 1 and EVA 2 samples, respectively. This type of analysis provided the amount of vinyl acetate present in a copolymer such as Ethylene-Vinyl Acetate. The results of both samples show decomposition at temperatures between 393 °C and 496 °C. In addition, both samples display a decomposition curve in several stages with no stable intervals. These results agree with the literature for the decomposition pattern of vinyl acetate, which occurs in the first stage (350-400 °C). The amount of vinyl acetate for EVA 1 corresponds to 12.43% and for EVA 2 to 26.83%.

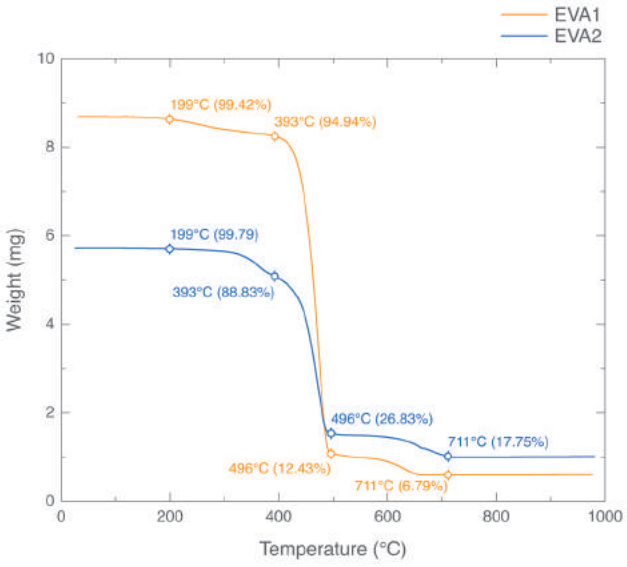

Figure 2. *Comparative TGA graph of EVA samples.*

DSC Analysis

Figure 3 shows the DSC curves of the EVA 1 and EVA 2 samples respectively, obtained with a heating ramp of 20° C/min from room temperature up to 150° C. The most intense peak in the EVA 1 sample occurs at a temperature around 116° C and corresponds to an endothermic fusion in the compound (starting at about 70° C). This corresponds to the onset for melting of the Ethylene-Vinyl Acetate copolymer. EVA 2 presents changes of enthalpy before 80° C, however, there is no defined peak as in EVA 1.

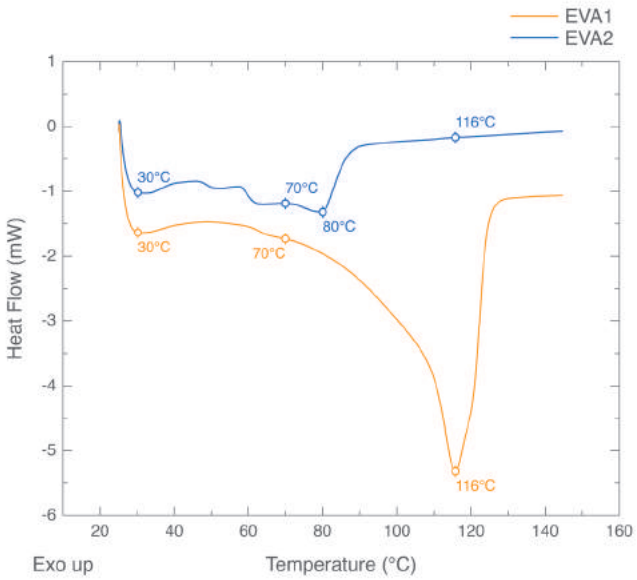

Figure 3. *Comparative DSC plot of EVA samples.*

Journal of ENGINEERING in Medical Devices

FTIR Analysis

According to Figure 4, it is notorious that the main differences occur between 2000 cm^{-1} and 1500 cm^{-1}, where two notable peaks are detected in the EVA 2 sample. These peaks are due to the detection of the extremely polar covalent bonds of the compounds. Peaks located between 3000 cm^{-1} and 2750 cm^{-1} show a strong polar covalent bond corresponding to bonds between C-H and O-H. In addition, a peak of medium polar intensity can be observed in the EVA 2 sample near 1750 cm^{-1}, which corresponds to the double bonds of C-C and C-O.

It is also important to mention that the "fingerprint" zone (between 1400 cm^{-1} and 600 cm^{-1}) of the graph shows a peak of medium intensity and 2 peaks of low intensity in the EVA 2 sample, corresponding to the single bonds between C-C and C-O, respectively, while for EVA 1 only a medium intensity peak and several almost undetectable peaks were found.

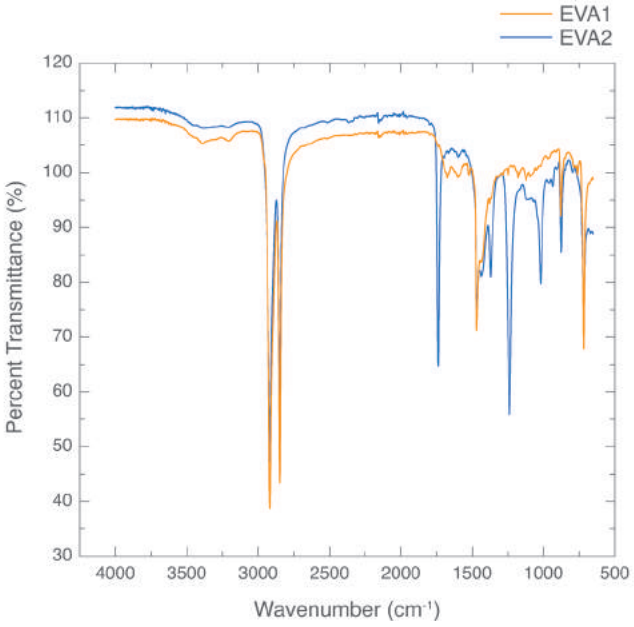

Figure 4. *Comparative FTIR graph of EVA samples.*

SEM Analysis

The images in Figure 5a and 5b correspond to scanning electron micrographs of the EVA 1 and EVA 2 samples, respectively, with a scale corresponding to a magnification of 250x.

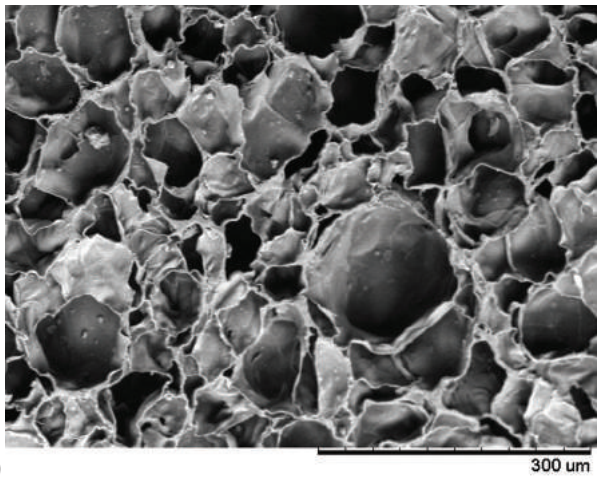

a)

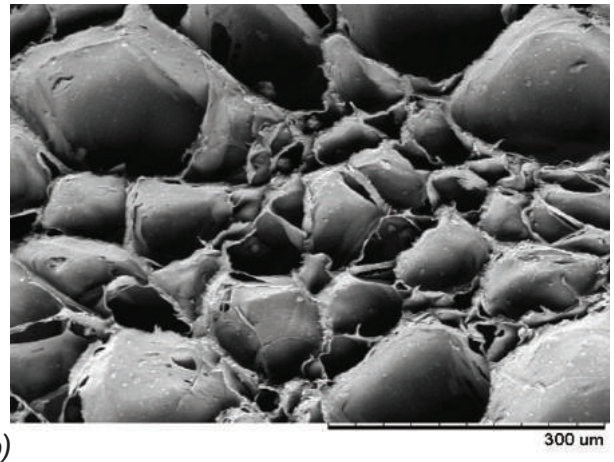

b)

Figure 5. *SEM micrographs of both EVA samples. a) EVA 1 and b) EVA 2.*

Using the linear intercept method, the cell size was obtained for both samples. The procedure followed for the calculations can be seen in Figure 6. Horizontal and vertical lines were drawn onto the micrographs, and the total number of intersections of the lines with cell borders were count. For the EVA 1 sample, the total horizontal length was 17.85 µm, with 385 intersections for an average cell size of 46.4 µm. In the vertical axis, the total length was 17.60 µm, with 419 intersections for an average 42.0 µm. For the EVA 2 sample, the total intercepts in the horizontal direction were 282, for an average cell size of 63.3 µm. Vertically, the total number of intercepts was 335, resulting in an average cell size of 52.5 µm. The aspect ratio of the cells was then 1.1 and 1.2 for the EVA1 and EVA2 samples respectively, which can be considered equiaxed.

A reduction of 27% of the cell size was seen in the horizontal direction, and of 19% in the vertical axis, from EVA 2 with respect to EVA 1.

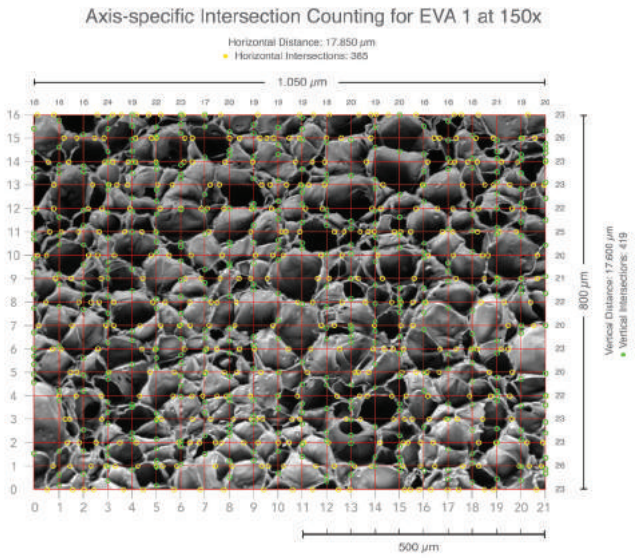

a)

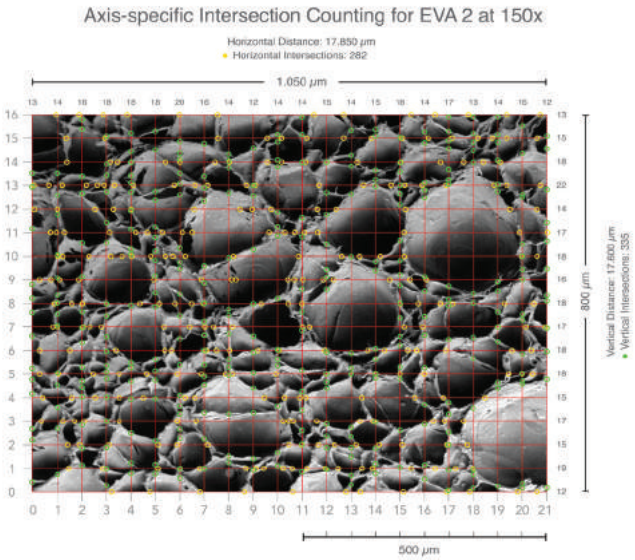

b)

Figure 6. *Lineal intercept method for EVA samples at 150x. a) EVA 1 and b) EVA 2.*

DISCUSSION

The XRD analysis identified $CaCO_3$ as a component of the sample. $CaCO_3$ has been used in the industry of orthopedic medical devices; being part of the formulation of bone cements for bone repair, prosthesis manufacturing and as a component of controlled drug release systems [7]. Additionally, literature reports that this compound has been used for the improvement of the mechanical resistance of materials [8], for this reason it can be inferred that it was added to the orthopedic insoles formula. It is important to underline that the component is present in both samples tested and the test does not provide information of concentration, therefore it is not possible to confirm that $CaCO_3$ is the responsible for the different levels of hardness of the material.

The most significant difference between the EVA diffraction in the EVA 1 and EVA 2 samples was the intensity of the emission, being stronger the (110) plane in EVA 1; which is affected by the collective scattering of all the atoms in the crystal, but it does not represent a significant difference between the samples. The structure of EVA detected corresponds to a cubic crystalline structure [9].

The TGA analysis showed a process with decomposition temperatures equal to the ones reported in the literature for Ethylene-Vinyl Acetate, and occurs in two phases. The first one is at approximately 350° C and corresponds to the loss of acetic acid; which is 20% of the vinyl acetate weight. This compound is reported to have a direct impact on the mechanical behavior of the polymer, being typically used to increase the flexibility of the materials [10]. In the second mass change, around 500-650° C, the acetic acid has been totally lost and the polymer backbone is decomposed releasing hydrocarbons.

The melting temperature of EVA was determined with DSC test as 72° C, which seems to correspond to the EVA 2 sample, since EVA 1 seems to have a much higher melting temperature. Because of this it can be concluded that EVA 1 is thermally more stable than EVA 2. However, is necessary to per-

form additional tests to determine the reason for these differences.

Using the FT-IR analysis it was determined that both samples have strongly polar covalent bonds, corresponding to C-H bonds; in addition, EVA 2 sample has a medium polar intensity peak near to 1750 cm^{-1}, which corresponds to the acetic acid bond. The FT-IR test had the limitation that the fingerprint zone was not compared to a database, therefore an integral analysis of the results that reveals other possible compound(s) in the samples is not available.

The SEM analysis allowed to observe the microstructure of the insoles and recognize the cellular structure. This structure can be achieved in the orthotics industry by adding a blowing agent to the Ethylene-Vinyl Acetate preparation, then heat is applied causing the blowing agent to evaporate and leave bubbles through the material.

The results obtained with the lineal intercept method previously discussed suggests that EVA 1 has the smaller cell size of both samples, providing evidence that, either the blowing agent was different for each sample or, that the blowing agent time was shorter for EVA 1 than for EVA 2. The uniformity of the size of the cells can be inferred from the SEM images. Comparing Figure 5a with Figure 5b, one can see that EVA 1 has more uniformity of cell sizes. These are important features to analyze since it can affect the properties of the material, therefore contributing to the differences of Shore hardness and thermal stability.

CONCLUSIONS

The results showed that the main compound present in the samples corresponds to Ethylene-Vinyl Acetate. Through XRD and TGA characterization techniques, it can be inferred that a higher presence of the vinyl acetate polymer (acetic acid + ethylene) increases the flexibility of the material, however it decreases the crystallinity of Ethylene-Vinyl Acetate.

Results obtained from TGA also determined that in the first decomposition of EVA 2, it lost more mass than EVA 1 under the same circumstances. Thus, according to the literature, EVA 2 has a higher concentration of vinyl acetate in its formulation than EVA 1.

Different Shore hardness between EVA 1 and EVA 2 may be affected by the size and uniformity of the cells of its structure. It was determined that the smaller and more uniform cell size was of EVA 1, corresponding to the highest Shore hardness. The concentration of $CaCO_3$ could also contribute to the hardness levels.

ACKNOWLEDGEMENTS

The authors are grateful to Laura Bolaños Chaves and Luis Alvarado Marchena for their assistance and guidance in carrying out the analyzes in the National Nanotechnology Laboratory (LANOTEC-CeNAT) and the Institutional Microscopy Laboratory of the Costa Rica Institute of Technology respectively, as well as Fisio Kinetics for providing all the Ethylene-Vinyl Acetate samples required to develop this research.

REFERENCES

[1] Root, M., Weed, J. and Orien, W. (1977) *Normal and Abnormal Function of the Foot*. (1st Ed.) California, United States of America: Clinical Biomechanics Corporation.

[2] Kirby, K. (2000) Biomechanics of the normal and abnormal foot, *Journal of the American Podiatric Medical Association*, 90(1), 30-35.

[3] Kilmartin, T. and Wallace, W. (1994) The scientific basis for the use of biomechanical foot orthoses in the treatment of lower limb sport injuries - A review of the literature, *British Journal of Sports Medicine*, 28(3), 180-184,.

[4] Drenth, J. (1999) *Principles of protein X-ray crystallography*. (2nd Ed.) New York, United States of America: Springer-Verlag.

[5] Leng, Y. (2013) *Materials Characterization: Introduction to Microscopic and Spectroscopic*

Methods, 2nd Ed. Weinheim, Germany: Wiley, 337-351.

[6] Wunderlich, B. (2005) *Thermal Analysis of Polymeric Materials*. Berlin, Germany: Springer Science & Business Media, 2005.

[7] Aragón-Fernández, J., González-Santos, R., Brizuela-Guerra, N., Oliver-Valdés, L. (2009) Estudio cinético de la liberación in vitro de un biomaterial compuesto por HAP- 200/POVIAC/ $CaCO_3$, *Revista Iberoamericana de Polímeros*. 10(2), 119-130.

[8] Betancourt, D., Martirena, F., Day, R. Díaz, D. (2007) The influence of the addition of calcium carbonate on the energy efficiency of fired clay bricks manufacture. *Revista Ingeniería de Construcción*, 22(3), 187-196.

[9] Yu, W., Sato, K., Wakabayashi, M., Nakaishi, T., Ko-Mitamura, E.P., Shima, Y., Urabe, I., Yomo, T. (2001) Synthesis of Functional Protein in Liposome. *Journal of Bioscience and Bioengineering*. 96(6), 590-593.

[10] Balart, R., López, J., García, D., Subiela, J., Vicente, F. (2007) Mechanical performance of composites based on Ethylene Vinyl-Acetate (EVA) matrix with powdered Zn filler, in: *Polymer and Biopolymer Analysis and Characterization*, 1st Ed. New York, United States of America: Nova Science Publishers Inc., 29-44.

Journal of ENGINEERING in Medical Devices

CHARACTERIZATION OF IMPURITIES IN 304 STAINLESS STEEL CABLES USED IN THE ASSEMBLY OF MEDICAL DEVICES

Wilber Mora[1], Giovanni Ramírez[2], Rita Rojas[3], Andrés Picado[4] & Jorge M. Cubero-Sesin[5]

Received: June 20th, 2017

Accepted: September 18th, 2017

1 Chemical Laboratorist, Bachelor, University Professor, University of Costa Rica, San José, Costa Rica, wilber.moraquesada@ucr.ac.cr

2 Chemical Laboratorist, Bachelor, Quality assurance analyst, University of Cost Rica, San José, Costa Rica, gioelequ@gmail.com

3 Biotechnology, Bachelor, Quality assurance analyst, Allergan, San José, Costa Rica, r18rojas@hotmail.es

4 Mechanical Engineer, Licensed, Transfer Engineer, Confluent, San José, Costa Rica, andrewpc2690@gmail.com

5 Professor, Ph.D., Center for Research and Extension in Materials (CIEMTEC), School of Materials Science and Engineering, Costa Rica Institute of Technology, Cartago, Costa Rica, jcubero@itcr.ac.cr

RESUMEN

Esta investigación muestra el estudio realizado sobre partículas presentes en cables de acero inoxidable 304 utilizados en el ensamblaje de dispositivos médicos. El estudio se realizó para desarrollar una caracterización superficial, química y térmica, que permita conocer la naturaleza de las impurezas. Se utilizó un análisis complementario utilizando diferentes técnicas como microscopía electrónica de barrido (SEM), espectroscopía dispersiva de energía (EDS), análisis termogravimétrico (TGA), calorimetría diferencial de barrido (DSC) y difracción de rayos X (XRD), para caracterizar las partículas, y concluir sobre su origen y su posible tratamiento. Los mejores resultados para el análisis se obtuvieron a partir de las imágenes generadas en el SEM, ya que, la naturaleza de la impureza resultó ser de carácter superficial, por lo que se pudo recomendar, como método de limpieza, el uso de solventes orgánicos.

ABSTRACT

This research shows a study of particles present in 304 stainless steel used in the assembly of medical devices. The study was performed in order to develop a superficial, chemical and thermal characterization, which allows to know the nature of the impurities. A complementary analysis using different techniques such as Scanning Electron Microscopy (SEM), Energy Dispersive Spectroscopy (EDS), Thermogravimetric Analysis (TGA), Differential Scanning Calorimetry (DSC), and X-Ray Diffraction Analysis (XRD) was used to characterize the particles, and to conclude on their origin and possible treatment. The best results for the analysis were obtained from the images generated in the SEM, since the nature of the impurity was superficial, so it was possible to recommend as a cleaning method the use of organic solvents.

Palabras Clave:

Dispositivos médicos, impurezas, caracterización, espectroscopía EDX, termogravimetría, calorimetría, microscopía, difracción de rayos-X.

Keywords:

Medical devices, impurities characterization, EDX spectroscopy, thermogravimetry, calorimetry, microscopy, X-ray diffraction.

Journal of ENGINEERING in Medical Devices

Introduction

The stranded wire tube is a component used for assembly of guidewires subsequently applied to manufacturing of some medical devices. Their assembly process is complex because it involves a wire drawing process and during this procedure, the chance of adding organic contaminants is quite high [1]

Due to the use of this material in the assembly of medical devices, it is extremely important that these components present low traces of any contaminants. Today there are a wide variety of characterization techniques that allow to gather information about a material. By scanning electron microscopy (SEM) it is possible to obtain information about the material structure and composition. It is also a good technique for analyzing a sample in terms of its topography doe to its large depth of field, which allows one to keep in focus much of the sample [2]. In the atomic interactions with the electron beam, some atoms of the sample are ionized, but this is an unstable energy state, so that the energy must be released as characteristic X-rays, with a determined wavelength for each element, which are collected in Energy Dispersive Spectroscopy (EDS).

Thermogravimetric analysis (TGA), provides a quantitative technique to determine the weight change of a material with temperature under heating. In dynamic processes, the weight change with respect to time (DTG) also provides valuable data for evaluating degradation [3]. In thermal degradation, it is logical to assume that the rate of decomposition is directly proportional to the amount of material present on the sample. Differential scanning calorimetry analysis (DSC), can show processes where an enthalpy variation occurs. This is appropriate to determine some physical characteristics in any material, for example determination of specific heats, boiling and melting points, purity in crystalline compounds and reaction enthalpies [4].

Chemical analysis by X-ray diffraction (XRD) is based on the fact that a crystalline substance always produces a characteristic diffraction pattern, a phenomenon that consists of the dispersion of X-rays by electron clouds surrounding crystal atoms, following a pattern that depends on the type of atom, the crystal structure and the wavelength of the X-rays. The observed pattern is the result of constructive and destructive interference of radiation scattered by all atoms [5].

The XRD technique is one of the most important in characterizing crystalline materials such as metals. This technique can be used to identify the phases present in the sample, as well as providing accurate information on the structure of materials. The quality of the diffraction pattern is usually limited by the nature and energy of radiation available for the resolution of the instrument and the physical and chemical conditions of the sample. Since many materials can be prepared only in a polycrystalline form, XRD becomes the only realistic option for a determination of the crystal structure of materials, and for this reason is that it offers an excellent platform to measure and identify complex phase mixtures that it can compare with a database.

In this technique, the most important phenomenon is that described by the Bragg Law, which indicates that if the wavelength of the X-rays is known and the diffraction angle (Theta) is measured, it is possible to determine the spacing of different atomic planes, and from them the crystalline structure for the diffracting material [5].

For the characterization analysis, the first step was a topographic visualization using the SEM to define the metallic surface and analyze if the impurity was part of the metallic structure, or otherwise a surface particle. Then, thermal analysis was carried out to show behavior differences between the metal and particles. The EDS and XRD analyses were used for the chemical and structural characterization of the unknown particles.

For this purpose, metallic cable samples were used, these samples presented problems during their incoming inspection and during their manufacturing process. This situation is of concern, because this material is used for medical device assembly. The purpose of this research was to use the various techniques described above to characterize the impurities present in the metallic cable, and determine

whether this contamination is organic or of another nature.

Materials and Methods:

For the determination of the nature of the impurity particles, the following characterization techniques were performed:

Scanning Electron Microscopy

Tabletop Hitachi TM-3000 and TM-1000 microscopes (Institutional Microscopy Laboratory, Costa Rica Institute of Technology) were used. The latter was coupled with an Energy Dispersive Spectroscopy (EDS) system. Images from the surface of samples were obtained at magnifications from 80X to 500X. For this purpose, an acceleration voltage of 15 KV was used. Samples with clean and dirty sections of the cable were analyzed by EDS, generating a chemical species spectrum.

Thermal Analysis

For the thermogravimetric analysis, a TA Q500 (National Nanotechnology Laboratory LANOTEC-CeNAT) instrument was used. A sample of the metallic cable of 15 mg was weighed in an alumina crucible for the analysis.

For differential scanning calorimetry (DSC) analysis a TA Q200 (National Nanotechnology Laboratory LANOTEC-CeNAT) was used. The measured mass of sample was ~30 mg on an aluminum pan. It was processed using a flow of Nitrogen gas of 50 mL/min and a temperature ramp of 20 °C/min from -89.98 °C to 396.98 °C.

X-Ray Diffraction Analysis

For the XRD technique, the sample was prepared by grinding so that multiple planes of the metallic structure are present in different angles when mounted on the holder, as shown in Figure 1.

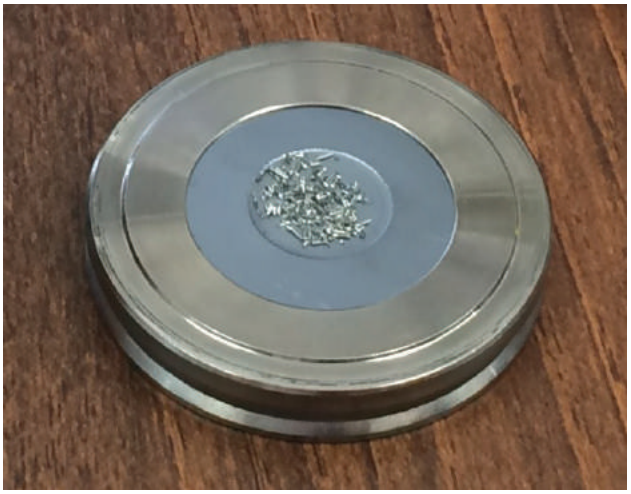

Figure 1. Sample placement on the silicon sample holder for the x-ray diffractometer.

The XRD was carried out in a Panalytical Empyrean powder diffractometer (School of Materials Science and Engineering, Costa Rica Institute of Technology). The parameters for analysis are shown in Table 1. The obtained spectrum was compared with the crystal structure databases in order to know the chemical nature of the sample and analyze its structure.

Table 1. *Parameter for X-Ray analysis*

Parameter	Value
Initial Position	5.0117 [º2Th.]
Ending Position	69.9857 [º2Th.]
Step size	0.0130 [º2Th.]
Scanning Time	3.5700 s
Generator setting	40mA, 45 KV
Scan Type	Continuous
Specimen Length	10.00mm
Measurement temperature	25 ºC
Anode material	Cu

Journal of ENGINEERING in Medical Devices

Results

Scanning Electron Microscopy

In the SEM analysis, the sample was observed at lower magnifications for a general visualization of the cable, then the image was magnified near to the sample surface and this allowed a detailed analysis of the sample topography. Besides it could be seen that the impurities show an irregular surface, as shown in Figures 2 a, b and c.

Figure 2a shows the cable has a high density of particles in dark contrast, and most of them are not visible to the human eye. The wire contains a lot of particles with different sizes and shapes and only the bigger ones are visible without a SEM. The particles become visible when they accumulate in the space between the wires of the coil.

Figure 2b shows a higher magnification view and allows to visualize that the particles are not part of the cable, and are rather external to the metal of the wire. The image also allows to determine that the size of impurity particles is not larger than 500 mm in length, most of them are in the order of 100 mm or less and it is observed that the impurity has not a regular form. Figure 2c shows a high magnification image of one such particles with a size of approx. 200 mm. Moreover, it confirms that the particle is of irregular shape.

Energy Dispersive Spectroscopy Analysis

The EDS analysis allows to make a scan on the sample, to determine the chemical elements presents in the material, this procedure can be performed during the SEM analysis, and generates a quasi-quantitative criteria about the composition differences between the samples. Figure 3 shows a comparison of the chemical composition of samples with and without impurities, in order to know their chemical nature.

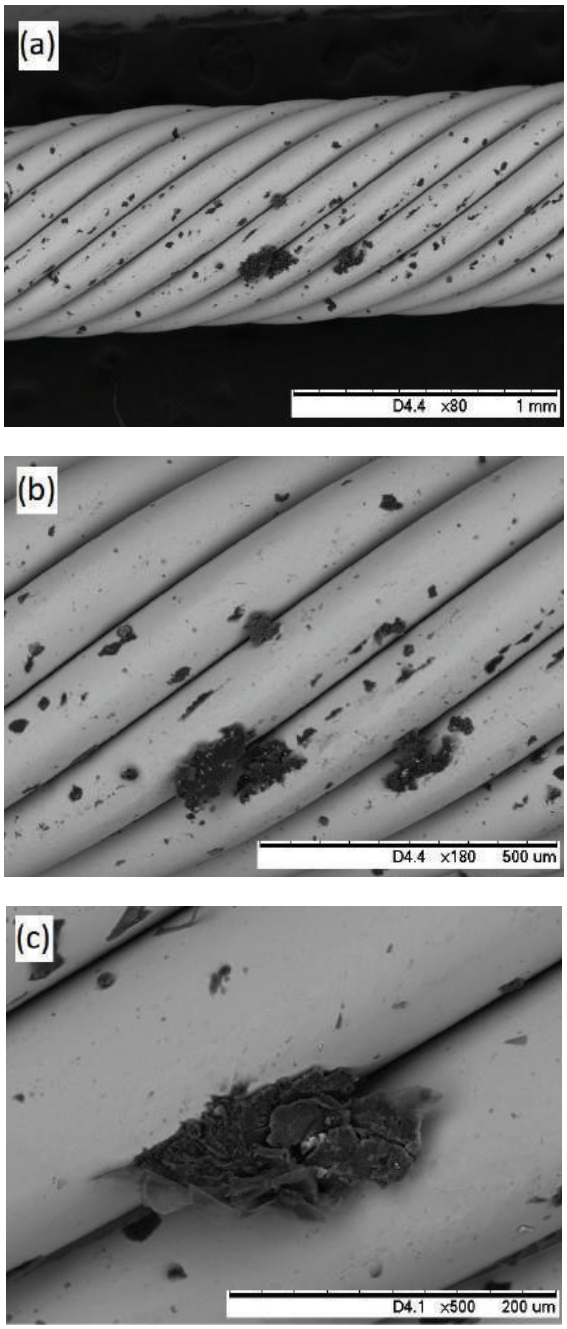

Figure 2. SEM image of the sample cable, at a) 80X, b) 180X and c) 500X.

The result shows that the contaminated sections of the wires have a major percentage of carbonic charge (6.5%) and in contrast to the clean section, it contains 0.5% of Chlorine, among other differences in the percentage of the components corresponding to the metal matrix.

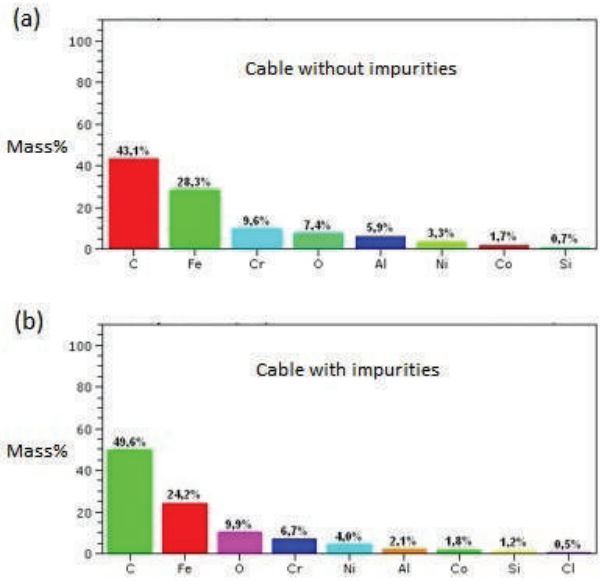

Figure 3. Comparison of the elemental composition in mass percent, between the cables (a) without and(b) with impurities by EDS Analysis

Thermal Analysis

For this analysis only cables with impurities were used. In the TGA instrument, the sample was heated in continuous way, from room temperature until 1000 °C, and the curve that exhibits the change of the sample mass versus of the heating temperature is recorded, as shown in Figure 4. The curve shows information of the reactions occurring in the sample involving loss or gain of mass. A slight decrease in the mass of 0.36% was recorded up to 400 °C, which indicates that some matter foreign to the cable is decomposing (volatiles), since the melting temperature of the cable is much higher. After this point, there is some gain in the mass of 0.9912% after 600 °C, possibly due to oxidation in the cable. There is some abnormal noise after 750 °C, but this is perceptible as product of the oxidation reaction, but also could be due to an external disturbance (noise) in the instrument.

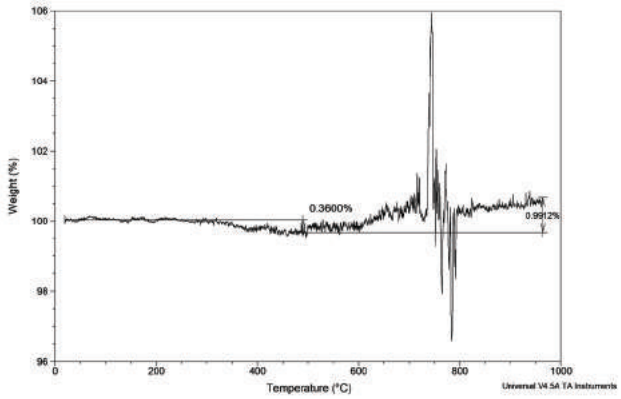

Figure 4. Thermogram of the sample cable by TGA analysis.

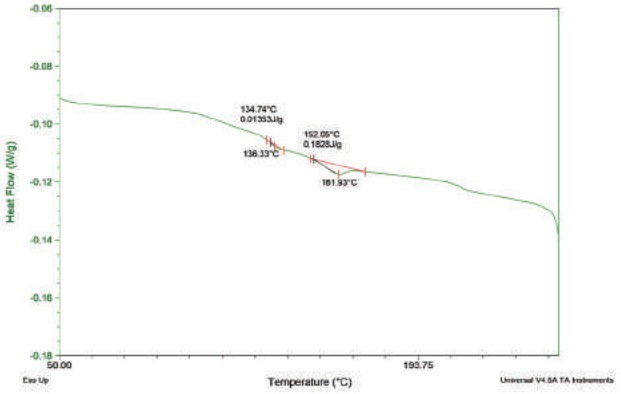

Figure 5. Calorimetric curve of the sample cable by DSC analysis.

The DSC analysis was carried out to measure the change in the reaction heat (enthalpy) with temperature. For this purpose, the instrument increases the sample temperature from room to 250 °C and calculates the reaction heat necessary to keep the sample at the furnace temperature, which is affected by the reactions occurring in the sample. This allows analysis of the different processes that alter the sample that don't involve changes in its mass.

It can be seen in Figure 5 that at least two endothermic reactions occurred at ~136 °C and ~162 °C, which is consistent with reactions in organic matter.

X-Ray Diffraction Analysis

The diffractogram in Figure 6 shows the results of a scan over the sample and registers the signals from X-rays that return to the detector versus the diffraction angle 2 θ.

Journal of ENGINEERING in Medical Devices

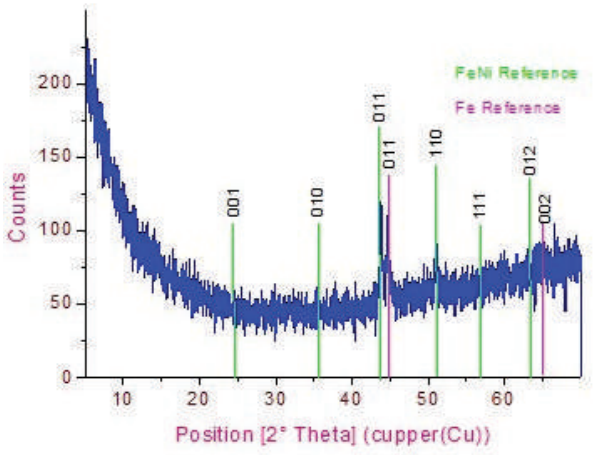

Figure 6. Spectrum for the sample cable by X-Ray Diffraction analysis.

In this spectrum, it is shown that the diffraction for the sample has a high noise signal that acts like interference in the results obtained, because the wavelength of Cu tube produces a high noise signal with ferrous samples. It has two maxima, which are near of the 45° and 50° (2Theta) respectively. The intensities for the rest of the diffraction peaks are low, and indeed it is difficult to distinguish between the signal of the sample and the noise signal. Nonetheless, diffraction from the Fe and $Fe_{0.612}Ni_{0.388}$ solid solution phases was detected by the XRD. The Miller indices (hkl) for the corresponding phases are shown in Figure 6, so that direct comparison can be made between the lines of maximum diffraction of the sample and the reference pattern. Table 3 shows the diffraction maxima from the reference patterns as extracted from the database, with the peak list of the "h", "k" and "l" values for the corresponding diffraction peak.

Table 3. *Comparison between the degrees and the orientation for the sample, and the $Fe_{0.612}Ni_{0.388}$ and Fe reference patterns.*

Sample	Orientation	2 Theta (deg)
Reference 98-010-8555 of $Fe_{0.612}Ni_{0.388}$	(001) (010) (011) (110) (111) (012)	24.858 35.438 43.772 50.987 57.531 63.630
Reference 98-063-1724 of Fe	(011) (002)	44.680 65.033

Through the characterization made by x-ray diffraction it can be said that the crystalline phases present in the wire are in agreement with the crystallographic references 98- 010-8455 for FeNi, with a tetragonal structure, and 98-063-1724 for Fe, with a body-centered cubic structure. However, other phases could be present that are not detectable by the XRD analysis due to the low signal to noise ratio.

Discussion

The SEM images in Figure 2 show that contamination can be distinguished, because the production of back-scattered electrons involved in forming the image vary according to atomic number, in that elements with different atomic number produce different amounts of backscattered electrons, so that the detectors pick greater intensity on substances with higher atomic number, such as the metal in the wire, and therefore display a bright contrast. Organic contamination is formed by low atomic number elements, such as in hydrocarbons, and they produce a darker contrast [6].

In the SEM technique, the radiation used is a monochromatic electron beam of high frequency, which generates good resolution at high magnification, and large depth of focus, and this allows perceive the impurity particle surface and volume in the analysis [2]. With the SEM analysis, it is noted that the contamination is present around all wires, and it is probably composed of organic compounds,

because their contrast is different of that from the metallic compounds in the wire.

The EDS analysis shown in Figure 3 indicates that the wires had a large fraction of carbon, and this amount increased in the contaminated area of the sample. Therefore, considering the SEM results it is correct to assume carbon is associated with the particles. In the EDS analysis, the incident radiation penetrates the sample and interacts with its atoms. For this reason, it is possible to detect emission spectra from both metallic and organic elements [7]. The elements present in the wire such as Fe, C, Cr, Ni, Al and Co were detected, so that others such as excess C and Cl are possibly due to external contamination. The composition results from EDS analysis, are not absolute, because O, C and Si are common elements present in the metal itself. From these elements, it is difficult to indicate with certainty what is the composition of the contaminant particles. A complimentary analysis such as FTIR spectroscopy could determine the specific composition [8].

In the thermogravimetry shown in Figure 4, it was possible to detect a loss of 0.36% mass after 300 °C, which although small, could be attributed to decomposition of organic particles, since this temperature is too low for the metal to show any transitions. After 600 °C there is a slight increase in mass, followed by a transition at 750 °C, probably produced by an oxidation reaction that occurs at elevated temperatures with the residual humidity in the sample chamber, resulting in an increase of ~1% in weight. It is important to mention that the TGA analysis may be affected by different error sources, so the sharp peak at 750 °C could also be due to buoyancy effects produced by the heat on gas or by the formation of foam, or a fluctuation in the flow gas [9].

Figure 5 shows the calorimetric curve for the metallic cable. It can be observed that there is a decrease in the heat flow with respect to the temperature steadily. This phenomenon occurs by a constant loss of heat capacity in the sample. Besides this, two endothermic transitions are observed at 134.74 °C and 152.05 °C (onset temperature), corresponding to enthalpies of 0.01353 J/g and 0.1828 J/g, respectively.

In general, the DSC can work in a temperature range ranging from liquid nitrogen temperature to about 600 °C, therefore this analytical technique is used to characterize materials that undergo thermal transitions in that temperature range. The type of materials that show all thermal transitions in this interval are polymers and organic materials. For example, the melting point for the stainless steel is around of 1400 °C [10]. Therefore, it is assumed that the transitions in Figure 5 are due to the organic particles on the wires.

From the diffraction pattern in Figure 6 it can be said that the phases detected by the XRD are characteristic of stainless steel [8]. The wavelength of the characteristic radiation depends on the material from the tube, and this has an important effect on the signal noise depending on the nature of the material to be analyzed. To work with most materials, Cu is recommended as the source, however, for ferrous materials such as Fe, Co is preferred because it generates less fluorescent scattering from the sample. Since for this analysis the sample was tested with a Cu tube and the material of the sample is stainless steel 304, there is a significant fluorescence from the sample getting into the detector. Although it was possible to obtain a spectrum, relatively high background radiation was produced, as shown in Figure 6. Nevertheless, the XRD showed results only about of the structure of the metal, but not from any other crystalline compound. Thus, it can be inferred that the structure of the particles is not crystalline, which is common for organic particles to have an amorphous structure [10].

It must be mentioned that most of the characterization techniques used in this research, indicate that the impurity is of organic nature, so that it is recommended to apply a cleaning process to the wire with an organic solvent, in order to remove the impurities. These particles could be produced by remnants of lubricants or debris in the manufacturing process, which is then passed on to the coiling operation, it could come from a previous process, before putting all the wires into a coil.

Conclusions

- Using the SEM technique, the most important visual information was collected. This analysis confirmed that the impurities have a low molecular weight and that they are at a superficial level, not embedded in the material.
- By the TGA analysis a slight decrease in the mass at low temperatures confirms the decomposition of some matter foreign to the wire. This was confirmed by endothermic reactions in the temperature range below 300 °C.
- The XRD did not show crystalline components besides those corresponding to the stainless steel. According to the analysis, the wire has a FeNi phase with a tetragonal structure, and an Fe phase with a cubic structure.
- In general, the characterization indicated that the impurities in the cable are of organic nature and are not part of the metal structure. An FT-IR analysis is recommended to isolated particles because the metallic matrix is an interference.
- It is recommended to clean the cable with some organic solvents or mild acids to remove the contaminants from the metal surface.

Acknowledgements

The authors are grateful to Felipe Orozco from the National Nanotechnology Laboratory (LANOTEC-CeNAT), to Esteban Rodríguez from the Center for Research and Extension in Materials (CIEMTEC) of the Costa Rica Institute of Technology, and to Luis Alvarado Marchena from the Institutional Microscopy Laboratory of the Costa Rica Institute of Technology, for their assistance and guidance in carrying out the analyses.

References

[1] Gálvez, F., Atienza J. M., Ruiz, J., Elices, M. (2001). Influencia de la velocidad de deformación en el comportamiento mecánico de alambres de acero trefilados. *Anales de Mecánica de la Fractura*, 18, 185-189.

[2] Goldstein, J.I., Newbury, D.E., Echlin, P., Joy, D.C., Romig, A. D., Charles, E.L., Lifshin, E. (1992). *Scanning Electron Microscopy and X-Ray Microanalysis.* Second edition. Springer Science + Business Media New York., 671-675.

[3] Barrera, J.E., Rodríguez, J. A., Perilla, J.E., Algecira, N.A. (2007). A study of poly (vinyl alcohol) thermal degradation by thermogravimetry and differential thermogravimetry. *Revista ingeniería e investigación*. 27(2), 100-105.

[4] Kodre K.V., Attarde S.R., Yendhe P.R., Patil R.Y., and Barge V.U. (2014) Differential Scanning Calorimetry: A Review. *Research & Reviews: Journal of Pharmaceutical Analysis*, 3(3), 11-22.

[5] Jenkins, R. (2000). X-ray Techniques: Overview. *Encyclopedia of Analytical Chemistry*, R.A. Meyers (Ed.), John Wiley & Sons Ltd, Chichester, 13269–13288.

[6] Melgarejo, J., Proenza, J., Galí, S., & Llovet, X. (2010). Técnicas de caracterización mineral y su aplicación en exploración y explotación minera. *Boletín de la Sociedad Geológica Mexicana*. 62(1) 1-23.

[7] Garratt-Reed, A., & Bell, D. (2003). *Energy-Dispersive X-Ray Analysis in the Electron Microscope*. First Edition. BIOS Scientific Publisher Limited. 5-6.

[8] ASM International (2003). *Characterization and Failure Analysis of Plastics*. ASM International Handbooks, Materials Park, OH, 364.

[9] Widmann, G. (2001). *Interpretation of TG curves*. METTER TOLEDO, USERCOM 1, 1.

[10] Loadman, M. (1998). *Analysis of Rubber and Rubber-like Polymers*. Fourth edition. Kluwer Academy Publishers, 163.

Computational Simulation of Severe Plastic Deformation:

Equal-Channel Angular Pressing (ECAP) processing of biomedical Ti-6Al-7Nb alloy.

David Carballo-Jarquín[1], Joaquín González-Hernández[2], Jorge M. Cubero-Sesin[3]

Received: August 22nd, 2017

Accepted: September 18th, 2017

1 Simulation Engineer, Emerson Electric, San José 10201, Costa Rica. davidcarba05@gmail.com

2 Professor, School of Materials Science and Engineering, Costa Rica Institute of Technology, Cartago, Costa Rica, jegonzalez@itcr.ac.cr

3 Professor, Ph.D., Center for Research and Extension in Materials (CIEMTEC), School of Materials Science and Engineering, Costa Rica Institute of Technology, Cartago, Costa Rica, jcubero@itcr.ac.cr

Journal of ENGINEERING in Medical Devices

ABSTRACT

Severe Plastic Deformation (SPD) techniques provide bulk materials with improved mechanical properties due to the ultrafine-grained (UFG) microstructures that can be achieved by this process. One of the most used and investigated methods of SPD is Equal-Channel Angular Pressing (ECAP). The deformation behaviour and characteristics of the material during the processing, have been researched with simulation software. The software contributes with the visual aid and the calculations of stress and strain. The information retrieved from simulations is necessary to complement experimental work and provide perspective in order to design the tools used in ECAP. This study presents a simulation of ECAP processing of commercial Ti-6Al-7Nb alloy.

RESUMEN

Las técnicas de deformación plástica severa (SPD, por sus siglas en inglés) producen materiales volumétricos con propiedades mecánicas superiores debido a microestructuras de tamaño de grano ultrafino (UFG, por sus siglas en inglés) que pueden desarrollarse con estas técnicas. Una de las más utilizadas e investigadas en SPD es la extrusión en canal angular constante (ECAP, por sus siglas en inglés). El comportamiento y características del material durante la deformación, han sido investigadas con software de simulación. El software contribuye con la ayuda visual y cálculos de esfuerzos y deformaciones. La información recuperada de las simulaciones es necesaria para complementar el trabajo experimental y provee perspectiva para diseñar las herramientas utilizadas en ECAP. Este estudio presenta una simulación del procesamiento por ECAP de una aleación comercial de Ti-6Al-7Nb.

Keywords:

severe plastic deformation, ultrafine-grained structure, equal-channel angular pressing, simulation, titanium-aluminum niobium

Palabras clave:

deformación plástica severa, estructura de grano ultrafino, extrusión en canal angular constante, simulación, titanio-aluminio niobio

Introduction

Severe plastic deformation (SPD) describes the effect of processing metallic alloys under a combination of extensive hydrostatic pressure and high deformations [1]. This process allows the formation of ultra-fine grains (UFG). The materials with UFG can be defined as polycristals with an average grain size under to ~1 **µ**m; also, most of these materials have a highly equiaxial and homogeneous microstructures, grain boundaries with high disorientation angles; this makes it possible to achieve unique properties in the material [2]. One of these properties is the biocompatibility.

Severe plastic deformation (SPD) describes the effect of processing metallic alloys under a combination of extensive hydrostatic pressure and high deformations [1]. This process allows the formation of ultra-fine grains (UFG). The materials with UFG structures can be defined as polycristals with an average grain size below ~1 **µ**m. Also, most of these materials have highly equiaxed and homogeneous microstructures, grain boundaries with high misorientation angles; this makes it possible to achieve unique properties in the material [2]. One of these properties is improved biocompatibility in biomedical titanium alloys [3]. To develop tools for SPD processes such as Equal-Channel Angular Pressing (ECAP), it is necessary to collect and generate information using numerical simulation.

The biomedical alloy Ti-6Al-7Nb, processed by SPD, is expected to increase its biocompatibility properties associate to osteo-conductivity, corrosion resistance and adhesion to tissues [3]. These properties enhance the range of applications in medical industry. The application of this kind of technology has not been officially implemented in the industry, since it still is in research and development stage.

One of the most important methods of SPD is ECAP [2]. ECAP is based on two intersecting channels of equal cross-section in an oblique angle [4]. The shearing stress the sample is subjected when it goes through the corner is the main source of deformation. The transversal section of the sample remains constant and it is possible to pass the same sample several times through the channel. Thus the process is accumulative, allowing high deformations rates [3].

In this work, simulations by FEM were done using CAE tools, to model the ECAP tooling used in the Materials Science and Engineering School of the Costa Rica Institute of Technology, specifically processing samples of Ti-6Al-7Nb through ECAP. Figure 1 presents a schematic representation of the ECAP process for the channel of 90° angle.

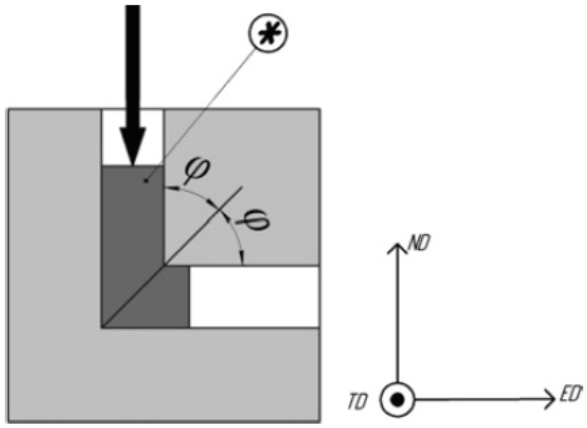

Figure 1. *Schematic of equal-channel angular pressing [3].*

General Objectives

Use finite element modeling tools to analyze the stress and strain behavior of the elements (samples and tools) during equal channel angular pressing.

Specific Objectives

- Model the geometry of the ECAP die used experimentally.
- Investigate the material properties, because the results of simulations are strongly linked to this data.
- Execute the simulations using Abaqus CAE software and analyze the results

Journal of ENGINEERING in Medical Devices

Justification

The general parameters and modelling conditions used are listed below as (a) and (b) respectively.

a) General Parameters

i. Material Properties:

The material properties for the alloy Ti-6Al-7Nb in the simulation models are:

- Density: 4.4x10-9 ton/mm^3.
- Young´s Modulus: 112 GPa
- Poisson Ratio: 0.3.
- Yield Strength: 847 MPa.
- Rupture Strength: 913 MPa at 8% of elongation.

ii. Geometry:

The ECAP process was simulated with two configurations. Figure 2 shows the schematic for the die, this specific design counts with two channels with either a 90° or 120° angle for deformation. Figure 3 presents the assembly for the ECAP models in both possible configurations for the die, left side 90° and right side 120°.

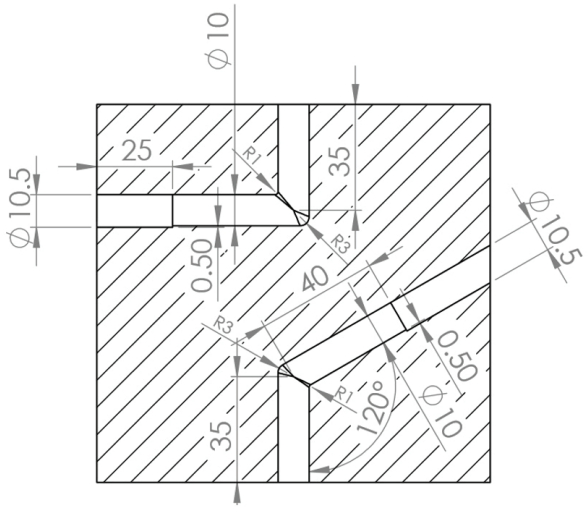

Figure 2. *Dimensions for ECAP channels*

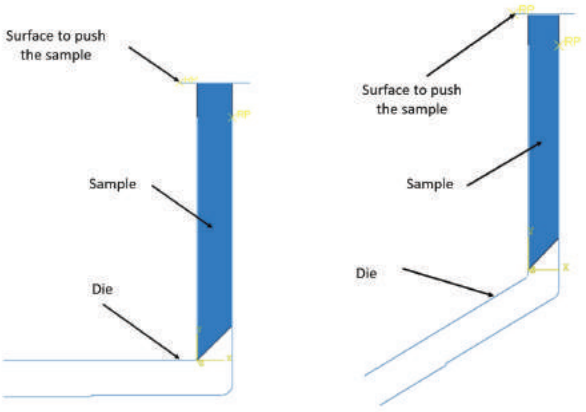

Figure 3. *Assembly for ECAP simulations.*

b) Model Conditions

i. Assumptions

- Dies and surfaces to push the samples are rigid surfaces (they weren't taken into consideration when the model was analyzed). By using rigid surfaces, the computational cost is reduced.
- The material properties are homogeneous in the samples of Ti-6Al-7Nb. Also, the material is assumed as perfectly isotropic.
- Heat transfer due to friction is negligible.
- In ECAP the friction coefficient is 0.1 in all contact surfaces [5].

ii. Boundary conditions for ECAP model:

- The die will be fixed during the whole simulation, this means, it will not have any degrees of freedom available for displacement.
- The surface to push the sample will only have the vertical degree of freedom available.
- All degrees of freedom will be available for the sample.

iii. Equation that governs the model:

- The equation that governs the analysis for ECAP in the linear range is Hooke´s Law:

  Where:

  : Stress.

: Young´s Modulus.

: Unitary Deformation.

iv. Mesh used in ECAP.

- The mesh used in the models is made of quadrilateral elements with complete linear integration.

State of the art

The ECAP results are shown in this section. The analysis performed provided information about the stresses in the die during the test. The contact study probes were located in the samples to check the highest stress points during the motion through the die. Figure 4 details the highest stress points by color code (blue: low, red: high).

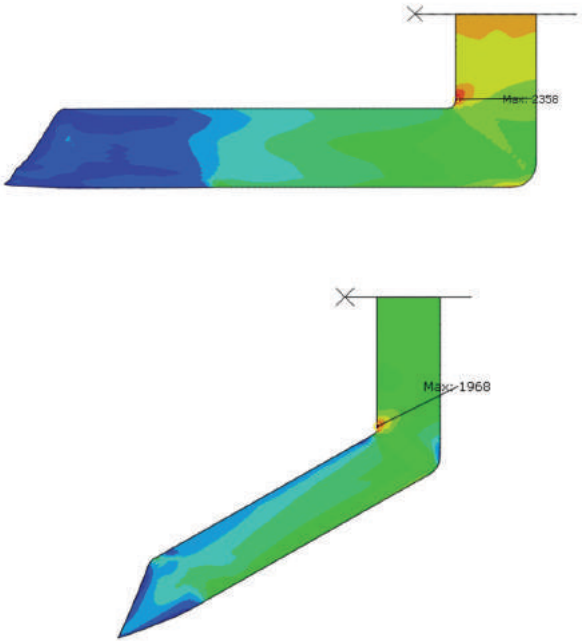

Figure 4. *Probes in areas with high contact pressure (units: MPa)*

Figure 5 is generated by using the contact pressure in the nodes shown in Figure 4 and the displacement of the surfaces to push the samples, which produces a graph of pressure vs displacement, meaning contact pressure and distance traveled by the probes.

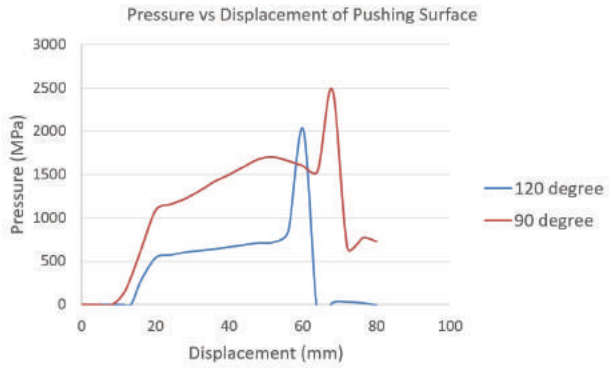

Figure 5. *Contact Pressure vs Pushing Surface.*

It is important to point out in Figure 5 that the die with 120º induces a decrease of around 20% in the contact pressure. In general, the shape of both curves is similar, but with an offset of 500 MPa. Regarding plastic deformation of the sample, for the 90º die, plastic deformation is higher, with zones approximately of 120% of permanent deformation. In the 120º die, areas with highest plastic deformation are only of around 60%.

Figure 6 shows plastic deformation of the sample for both 90º and 120º dies at 50% and 100% of motion through the die. Regarding material processing, this information shows higher deformation will be achieved with the 90º die.

Journal of ENGINEERING in Medical Devices

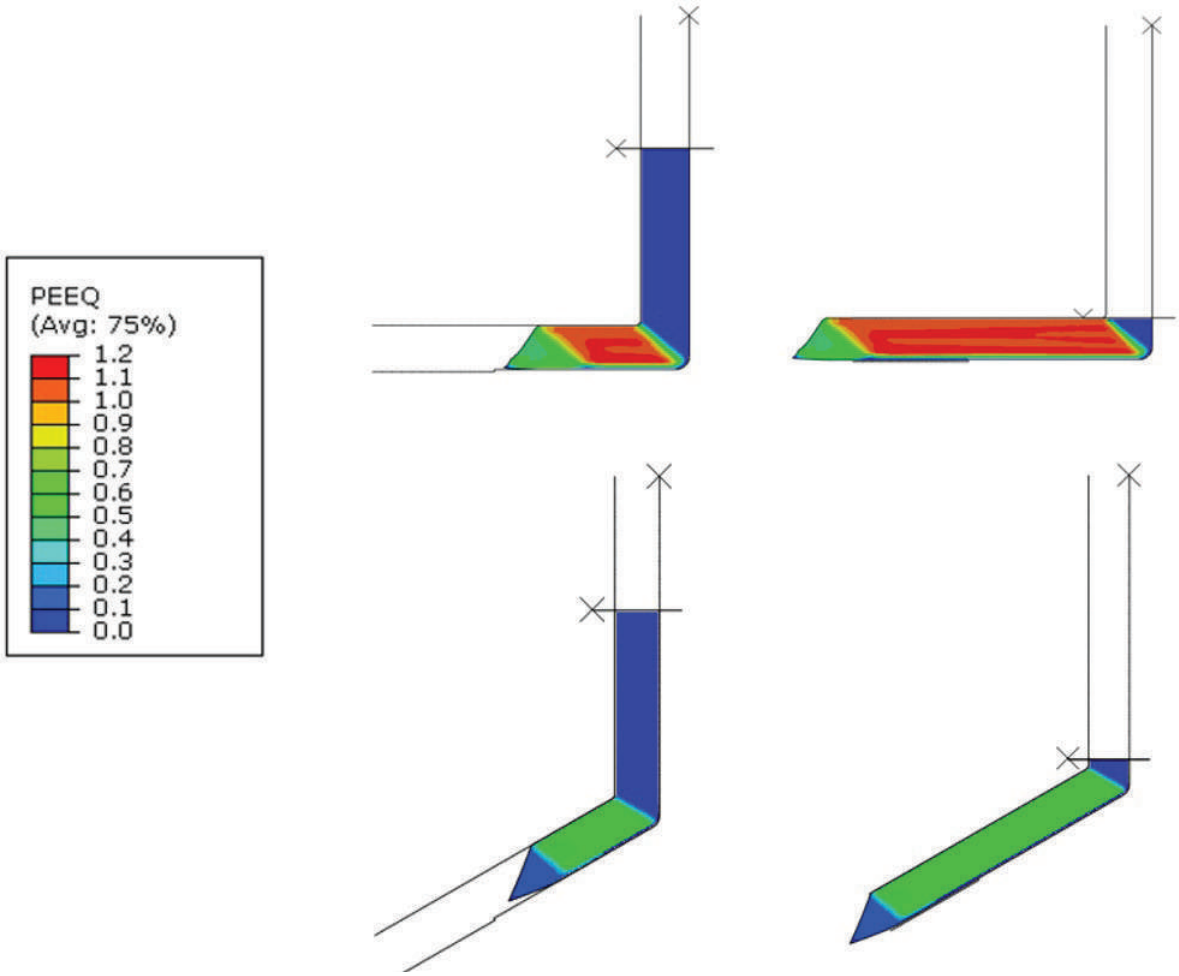

Figure 6. *Plastic Deformation. Source: Author.*

Finally, it is important to check the Von Mises stress in the simulation. Figure 7, shows that the process with a 90º die induces higher stresses in the sample; at 50% of travel, most of the sample has stresses above the yield strength of the alloy (847 MPa). With the 120º die, some areas are above the yield strength, however, the stresses are not as high in comparison with the 90º die.

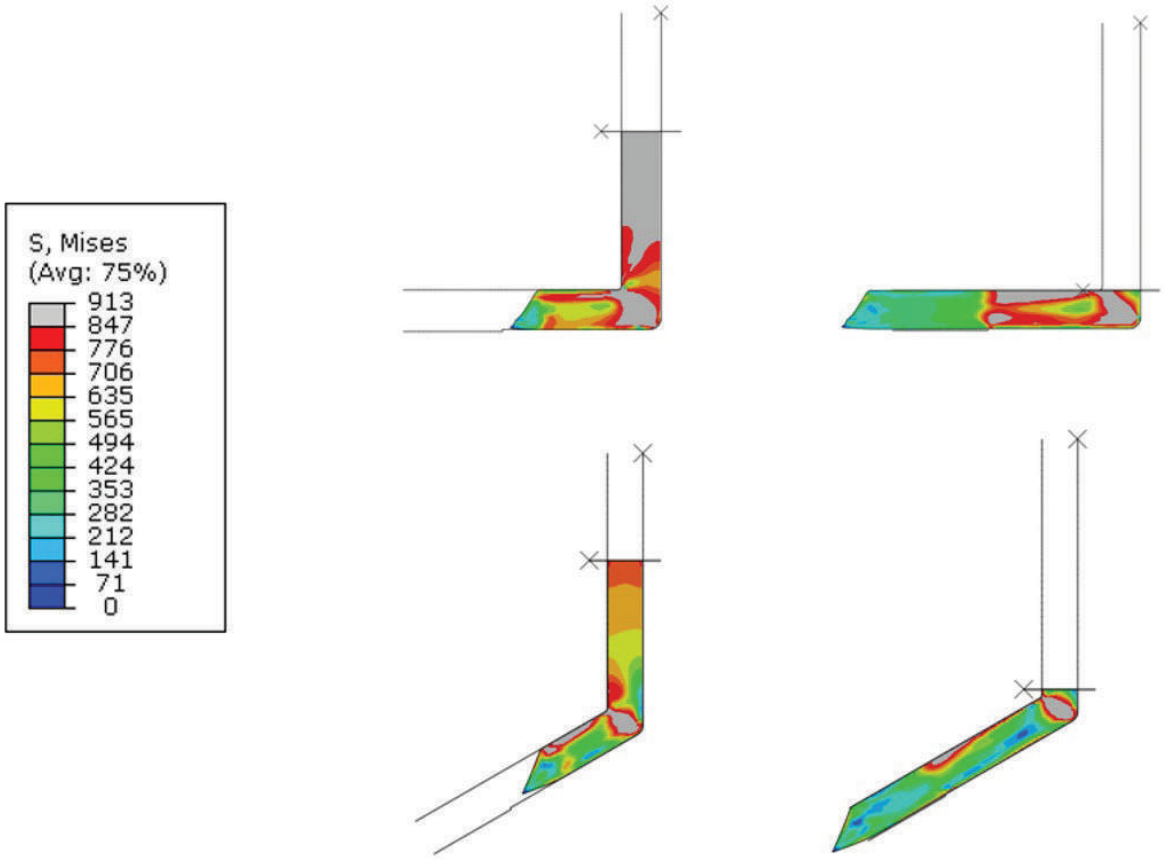

Figure 7. *Von Mises Stress.*

Conclusions

a) The 120º die will produce ~20% less load in comparison with the 90º die. This will produce less refinement in the crystalline structure. However, since the sample is refined by shear stress; big part of these stresses are originated from contact between the die and the sample; the greater the stresses, the greater the change in the crystalline structure.

b) The change in the grain size of the material due to ECAP will be more significant for the 90º die due to the higher stress and deformation from processing.

Acknowledgments

The authors acknowledge the support of Dr. Bruno Chinè, coordinator of the computational simulation lab of the Center for Research and Extension in Materials, School of Materials Science and Engineering, Costa Rica Institute of Technology. DC thanks the professors of the Master Degree Program of Medical Device Engineering of the Costa Rica Institute of Technology for support and advice.

References

[1] Khoddam, S., Hodgson, P., Zarei-Hanzaki, A. and Yan Foon, L. (2016) A simple model for material's strengthening under high pressure torsion, *Materials and Design*, 99, 335-340.

[2] Valiev, R.Z., Estrin, Y., Horita, Z., Langdon, T., Zehetbauer, M.J. and Zhu, Y.T. (2006) Producing Bulk Ultrafine-Grained Materials by Severe Plastic Deformation, *JOM*, 58(4), 33-39.

[3] Estrin, Y. and Vinogradov, A. (2013) Extreme grain refinement by severe plastic deformation: A wealth of challenging science, *Acta Materialia*, 61(3), 782-817.

[4] Kim, H.S. (2002) Evaluation of strain rate during equal-channel angular pressing, *Journal of Materials Research*, 17(1), 172-179.

[5] Yoon, S.C., Bok, C.H., Seo, M.H., Kim, T.S., Kim, H.S. (2008) Comparison in Deformation and Fracture Behavior of Magnesium during Equal Channel Angular Pressing by Experimental and Numerical Methods, *Materials Transactions*, 49(5), 963-966.

[6] ASTM International (2016) Standard Specification for Wrought Titanium-6Aluminum-7Niobium Alloy for Surgical Implant Applications (UNS R56700), ASTM-F1295-16.

[7] Niinomi, M. (1998) Mechanical properties of biomedical titanium alloys, *Materials Science & Engineering A*, 243(1-2), 231-236.

[8] Conejo-Herrera, M. (2016) Simulación del procesamiento de una aleación de Ti-6Al-7Nb por Equal-Channel Angular Pressing (ECAP) mediante el método de elementos finitos, *Lic. thesis*, Instituto Tecnológico de Costa Rica.

[9] Görtan, M. O. (2014) Severe plastic deformation of metallic materials by equal channel angular swaging: Theory, experiment and numerical simulation, Ph.D. thesis, Technische Universität, Darmstadt.

Bibliography

x S. Khoddam, P. Hodgson, A. Zarei-Hanzaki and L. Yan Foon, "A simple model for material's strengthening under high pressure torsion," p. 6, 2016.

[2] R. Valiev, Y. Estrin, Z. Horita, T. Langdon, M. Zehetbauer and Y. Zhu, "Producing Bulk Ultrafine-Grained Materials by Severe Plastic Deformation," p. 7, 2006.

[3] Y. Estrin and A. Vinogradov, "Extreme grain refinement by severe plastic deformation: A wealth of challenging science," p. 36, 2013.

[4] H. Kim, "Evaluation of strain rate during equal-channel angular pressing," *Department of Metallurgical Engineering, Chungnam National University, Korea,* p. 8, 2001.

[5] C. H. B. M. H. S. T.-S. K. H. S. K. Seung Chae Yoon, "Comparison in Deformation and Fracture Behavior of Magnesium during Equal Channel Angular Pressing by Experimental and Numerical Methods," *Materials Transactions,* vol. 49, pp. 963-966, 2008.

[6] A. International, Standard Specification for Wrought Titanium-6Aluminum-7Niobium Alloy for Surgical Implant Applications (UNS R56700), 2016.

[7] M. Niinomi, "Mechanical properties of biomedical titanium alloys," *Materials Science & Engineering,* pp. 231-236, 1998.

[8] M. C. Herrera, *Simulación del procesamiento de una aleación de TI-6AL-7NB por Equal-Channel Angular Pressing (ECAP) mediante el método de elementos finitos,* San José: Instituto Tecnológico de Costa Rica, 2016.

[9] M. O. Görtan, *Severe plastic deformation of metallic materials by equal channel angular swaging: Theory, experiment and numerical simulation,* Darmstadt: Technischen Universität Darmstadt, 2014.

Guidelines for publication

The journal is a biannual publication of the Master of Medical Devices of TEC, which links professionals in the fields of engineering and health sciences, and its main objective is to serve as a platform for the exchange of knowledge in this field.

All authors can submit their manuscript by sending it to the Editorial Director e-mail: jcubero@itcr.ac.cr. As soon as the paper is processed, the author will be contacted.

Receipt of a job does not imply any commitment to publication by the journal.

The Editorial Board will analyze and select the works according to the format and content criteria, seeking a contribution to the knowledge and scientific exchange of professionals in the field.

As the Editorial Board considers, the articles will be accepted or rejected, or revisions will be suggested prior to publication:

- Comments to the author or authors, indicating in their case, points to reconsider, explain or modify.

Structure and format for sending the articles

- Items must be submitted in English.
- The article should indicate the category of the publication. Applied Engineering, Academic Focus or Technical Note. It must be presented in text format (Microsoft Word .doc, Open Office .odt, etc.) written in Arial 12, double-spaced.

  The articules should not exceed fifteen thousand characters, without spaces and the maximun of ten figures.
- Images or photographs: Images must be sent in a separate file from the main document.

  They must have a minimum resolution of 300 dpi and the supported formats are PDF, JPG, TIF or EPS. They must be clearly identified with numbers to know their precise location in the main document.
- Graphics, tables, tables: can be included within the same file as the main document.

Structure of the article (for Applied Engineering or Academic Focus type of articles):

- Title: must be in Spanish and English, in affirmative, capitalized, bold and centered; Its maximum extension is ten words and in extreme case fifteen.
- Authors: immediately below title, sorted according to scientific contribution; The name and a single last name are noted; If both surnames are used, they must be joined by a hyphen. At the bottom of the page, with an asterisk or Arabic number to identify each author, the name, profession, academic degree, institutional position, city, country and e-mail address must be attached. Indicate the professional qualities (academic degree and name of the career that is taken in case of university students, or, the respective specialty). It must indicate the current position or position of each author.
- Spanish summary: 150 to 250 words in the third person.
- English abstract: must be a faithful translation of the Spanish summary.
- Keywords: both in the summary in Spanish and in the English abstract, must be from three to ten words; Only the use of nouns or affirmative sentences are allowed; It is not allowed to use adjectives, abbreviations, adverbs, synonyms, isolated verbs, conjunctions or articles; keywords will be written separated by a comma.
- Introduction: it presents what the researcher tries to reach, observe or measure, and why; Is written in the affirmative, subject to a single interpretation. It includes research questions, problem statement and justification, general context or background, critical or historical review of existing knowledge; The strategy or method that was used to solve the problem; The frame of reference or the concepts necessary to make clear the theoretical position of the author; should be strictly limited to the subject matter without extensive review. If it is a case study, it should justify publication with epidemiological or clinical arguments and their implications for public health, other reported cases are reviewed and articles and references are included.
- Material and method, or subjects and methods, in research articles: describes how the research was done; May consist of the following parts:
  - Design: mentions the premises and limitations, the instruments used, their validity and reliability, and the reason for their choice. When it comes to established and well-known methods, they are indicated by bibliographic citations; When they are new or modified methods, should be described in detail.
  - The population: details the size and the way in which the representative sample was selected, as well as the inclusion and exclusion criteria. The term "participants" is used when they are human, and the term "subjects" when dealing with non-human individuals.
  - The environment: indicates where the research was performed.
  - Interventions: explains the techniques required for the execution of the research or procedures performed, so that the experience can be reproduced. It also clarifies whether the procedures followed conform to national and international ethical standards, how the informed consent was obtained, and the record of the review of the investigation by an institution's board or ethics committee.
  - The analysis: details the strategies and procedures that will be used to analyze or process the data, results or information obtained. It should reflect that the statistical procedures used were correct; If the study has hypotheses, the approval or rejection of it should be clearly stipulated. If the study included study and control groups, these should be compared, indicating precisely the duration of the study (follow-up) for both. It should be considered whether the data were analyzed by qualitative, quantitative or both techniques and indicate the steps that were followed to validate the results.
- Results: the research question or the hypothesis test must be answered. It is recommended to present them in the order the objectives were set. The data must be presented in a specific form, without comments or arguments, or value judgments, nor justifications. Do not repeat all the data in the tables and figures, only summarize the most important, on the other hand, tables should not duplicate the text. In the writing of the results, perfect past tense must be used in impersonal construction ("discovered"), no first person singular or plural should ever be used.
- Discussion and comment, the answer to the question posed in the introduction is presented, followed by the tests shown in the results. Examine and interpret the results. It determines the coherence or contradictions of the data found within the context of current scientific knowledge, does not polemize in a trivial way.

- Conclusions: The contribution ends with one or several conclusions that are a synthesis of the discoveries, without drawing more conclusions than the results allow. In the case study, the main findings, particularities or contrasts should be counted. The conclusions are written in present tense ("these data indicate"). Recommendations may be included if appropriate.

Structure of technical notes

Technical notes should follow the same structure as regular articles up to the introduction section, then they should present the General Objective, Specific Objectives, Justification, State of the Art, followed by conclusions and references as in regular articles.

Acknowledgements

The authors can recognize any persons or organizations that provided support and/or funding to carry out the activities.

References

- Must be submitted according to APA format.
- All references presented in this section should be in order of citation in the text and must be cited somewhere in the text, using a number within square brackets, and presented in this section.
- The minimum number of references per contribution is 8.

Graphic elements:

- Tables: they should not bring vertical lines, only horizontal lines, and should cover the entire width between the left margin and the right margin.
    - Titles should be brief, clear and explanatory; Should be in italics, except for the word "Table" and the number that identifies it. The title, like the number, goes at the top of the table and no indentation.
- In the case study articles, use of x-rays, ultrasound, tables and comparative graphs is allowed. You can include three to five photographs, with their corresponding caption, the name of the case and a short description.

Article submission

Items must be sent to:
Jorge Cubero Sesin
Editorial Director: jcubero@itcr.ac.cr

TEC | Tecnológico de Costa Rica

MIDM

Maestría en Ingeniería en Dispositivos Médicos

MASTER PROGRAM IN MEDICAL DEVICES ENGINEERING IN COSTA RICA
SCHOOL OF MATERIALS SCIENCE AND ENGINEERING
COSTA RICA INSTITUTE OF TECHNOLOGY (TEC)

Our Program

Application Process for the Master Program in Medical Device Engineering (Class 2018)

We are very happy to announce the opening of the application process for admission to the 4th generation that will start class on January 2018. Application deadline is October 31st. The online form is available at:

Application form

Or refer to the QR Code below.

As we are looking forward into the 4th generation, changes to the program are being made to accommodate local industry requirements. Among them, an increase in the number of hours dedicated to understanding Regulation in the Medical Device Industry and how it applies to every aspect of the manufacturing process. A course on Anatomy and Physiology was added and the course of CAD CAM CAE has been restructured to accommodate practical laboratories that will be held at TEC installations. We have built up on our previous experience with RICE University students, to develop need finding activities at local hospitals to find topics for the graduation projects.

Our program includes courses on Regulation, Packaging and Sterilization, Design of Experiments, Metals and Polymer Processing, CAD-CAM-CAE, Prototype Design, Macro environment, Failure Analysis and Materials Characterization Techniques. There are two elective courses that students can take with the program from the topics of: Anatomy and Physiology, Advanced Simulation, Biocompatibility, Innovation and Plasma Applications.

For more information on the program visit our page at:

https://www.tec.ac.cr/programas-academicos/maestria-ingenieria-dispositivos-medicos

The link to the application form can also be found in the program website

FOR MORE INFORMATION

Ricardo Esquivel Isern
Program Coordinator
Master Degree in
Medical Device Engineering
Tecnológico de Costa Rica (TEC)
resquivel@itcr.ac.cr
(506) 2550-2705

Our Research Center

CENTER FOR MATERIALS RESEARCH AND EXTENSION (CIEMTEC)
SCHOOL OF MATERIALS SCIENCE AND ENGINEERING
COSTA RICA INSTITUTE OF TECHNOLOGY (TEC)

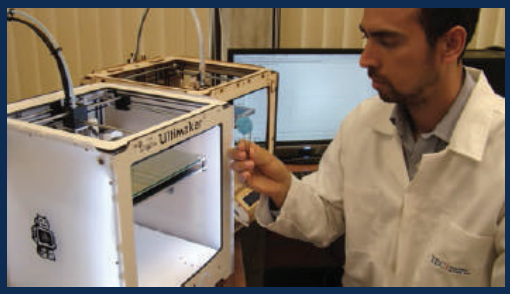

FOR MORE INFORMATION

José Luis León Salazar
Coordinator
Center for Materials Research and Extension (CIEMTEC)
Tecnológico de Costa Rica (TEC)
jlleon@itcr.ac.cr
(506) 2550-2384

This Center was founded in 1982 along with the Metallurgy program, in cooperation with the Italian government. The aim of this center was to give support and develop the activity of the metallurgical industry in Costa Rica. Now, the industry as well as our Center have evolved to include new materials and complex processes.

The Center covers three important areas: research, teaching and support to industry. In research, the center supports several projects:

- Application of non-destructive testing (NDT) for controlling the properties of porous and cellular materials (foams, sponges, etc.) for medical applications and radiation shielding.
- The characterization of defects and nanostructural alterations in the Nimonic 80A superalloy after the heat treatment and fatigue testing by transmission electron microscopy.
- Development of porous implants from biopolymers and hydroxyapatite by using 3D printing for bone implants.
- Development of nanostructured titanium alloys for biomedical applications by a severe plastic deformation (SPD) method known as High-Pressure Torsion (HPT) to achieve grain refinement to a nanostructure and therefore increase de mechanical strength above the levels of commercial alloys.
- Corrosion of concrete and degradation of its mechanicals properties by CO_2 which permeates the porous and fracture structure of the concrete, which is a fundamental issue for establishing conditions of the concrete degradation.
- Polymeric material degradation by irradiation.
- Development of materials for biosensors and electrochemical sensors for detection of contaminants.

The services provided to the industry include heat treatment, material testing and characterization such as hardness, micrographic analysis, chemical composition, x-ray diffraction, tensile testing, axial and torsional fatigue, straining, cross section analysis, coating thickness, among others. Failure analyses are the most common, as well as material behavior in different conditions. Although destructive testing is often required, the support in NDT is special in our Center, covering from training to inspection in metallic bridges, boilers, oil containers, oil pipes, port platforms, as well as quality control of welded structures in general.

Teaching is strengthened by the experience in research and support to industry. In our Center, undergraduate and graduate students can improve their skills, with workshops and laboratories to gain the experience they need to deal with the medical industry. Our graduate students work in projects with our research professors to find solutions in medical applications.

- Personalized trans-tibia prosthetic design implementations with additive manufacturing.
- Bioactive hydroxyapatite coatings on biopolymers by atmospheric plasma spray.
- Collagen and organic nanoparticle extracts for biomimetic tissue applications.
- Characterization of biomedical alloys with special microstructures for medical devices.

In the framework of the Doctorate Engineering program, there are two important projects which are carried out in the CIEMTEC:

- Application of crystal engineering technology to improve the solubility of drugs, such as Irbesartan and Lovastatin
- Development of an in-vitro system to be adaptable in dynamic mechanical testing machines in order to generate biomechanical stimuli on scaffolds.